© 2022. Published by The Company of Biologists Ltd | Development (2022) 149, dev200692. doi:10.1242/dev.200692

RESEARCH ARTICLE

Target-dependent suppression of siRNA production modulates the levels of endogenous siRNAs in the *Caenorhabditis elegans* germline

Zoran Gajic[1,*,¶], Diljeet Kaur[1,‡,¶], Julie Ni[1,¶], Zhaorong Zhu[1], Anna Zhebrun[1], Maria Gajic[1], Matthew Kim[1,§], Julia Hong[1], Monika Priyadarshini[2], Christian Frøkjær-Jensen[2] and Sam Gu[1,]**

ABSTRACT

Despite the prominent role of endo-siRNAs in transposon silencing, their expression is not limited to these 'nonself' DNA elements. Transcripts of protein-coding genes ('self' DNA) in some cases also produce endo-siRNAs in yeast, plants and animals. How cells distinguish these two populations of siRNAs to prevent unwanted silencing of active genes in animals is not well understood. To address this question, we inserted various self-gene or *gfp* fragments into an LTR retrotransposon that produces abundant siRNAs and examined the propensity of these gene fragments to produce ectopic siRNAs in the *Caenorhabditis elegans* germline. We found that fragments of germline genes are generally protected from production of ectopic siRNAs. This phenomenon, which we termed 'target-directed suppression of siRNA production' (or siRNA suppression), is dependent on the germline expression of target mRNA and requires germline P-granule components. We found that siRNA suppression can also occur in naturally produced endo-siRNAs. We suggest that siRNA suppression plays an important role in regulating siRNA expression and preventing self-genes from aberrant epigenetic silencing.

This article has an associated 'The people behind the papers' interview.

KEY WORDS: siRNA suppression, Genome surveillance, *C. elegans* germline, RNAi, Transposon

INTRODUCTION

Small RNAs, such as microRNAs, endogenous-small interfering RNAs (endo-siRNAs), and piwi-interacting RNAs (piRNAs) carry out a diverse set of cellular functions through their ability to silence homologous genes. Small RNAs orchestrate gene silencing by serving as guide molecules to bring the Argonaute (AGO) family of proteins and other regulatory proteins to the target RNA transcripts. Therefore, the steady state level of small RNAs is a key determinant of the gene silencing activity.

The endo-siRNA pathway in *Caenorhabditis elegans* germline is a powerful system to explore small RNA biology and transgenerational epigenetic inheritance (Billi et al., 2014). Among the different classes of endo-siRNAs, the ones that target transposons and other repetitive DNA elements belong to the secondary siRNA or 22G-RNA class (Gu et al., 2009), which are *de-novo* synthesized by RNA-dependent RNA polymerases (RdRPs) using the target mRNAs as the template. 22G-RNA synthesis can be triggered by a diverse set of RNA molecules/structures: dsRNA (Fire et al., 1998), 26G-RNA (Han et al., 2009; Gent et al., 2010), piRNA (Ashe et al., 2012; Lee et al., 2012), aberrant mRNA processing (Newman et al., 2018; Makeyeva et al., 2021) and untemplated RNA-tailing (Shukla et al., 2020). Once produced, these siRNAs are bound by the germline AGO proteins such as WAGO-1 (Gu et al., 2009) and HRDE-1 (Buckley et al., 2012), which induce post-transcriptional and transcriptional repression at the target genes. The steady state level of siRNAs is determined through both biogenesis and turnover of siRNAs. Recent studies have identified numerous biochemical activities that can affect the siRNA turnover rate, such as siRNA tailing (van Wolfswinkel et al., 2009; Pisacane and Halic, 2017; Zhou et al., 2017; Wang et al., 2020) and the stability and processing of AGO proteins (Batista et al., 2008; Gudipati et al., 2021). In these cases, it is unclear to what extent the siRNA turnover is mediated by their target mRNA.

Interestingly, actively transcribed germline genes also naturally produce 22G-class siRNAs in *C. elegans* (Claycomb et al., 2009; Maniar and Fire, 2011). For the purpose of this study, we refer to these siRNAs as self siRNAs and the ones from transposons as nonself siRNAs. Both populations are synthesized by RdRPs and share the same size distribution that peaks at 22 nt and the 5′ guanine bias. Despite these similarities, the self siRNAs differ from the nonself siRNAs in at least two aspects. First, self siRNAs have much lower density, as measured by normalized read count per unit length of mRNA, than nonself siRNAs (Fig. S1). Second, they are enriched in different AGO proteins: the nonself siRNAs in WAGO-1 and HRDE-1 and self siRNAs in another germline-specific AGO protein CSR-1 (Claycomb et al., 2009). Self siRNAs have been suggested to fine-tune germline gene expression: loss of the germline RdRP enzyme EGO-1 leads to reduced levels of self siRNAs and increased mRNA expression of the corresponding germline genes (Maniar and Fire, 2011); loss of the CSR-1 protein also leads to complex dysregulation of germline gene expression and ultimately sterility (Claycomb et al., 2009; Seth et al., 2013; Cecere et al., 2014; Campbell and Updike, 2015; Gerson-Gurwitz et al., 2016; Fassnacht et al., 2018).

[1]Department of Molecular Biology and Biochemistry, Rutgers, The State University of New Jersey, Piscataway, NJ 08854, USA. [2]Biological and Environmental Sciences and Engineering Division (BESE), King Abdullah University of Science and Technology (KAUST), Thuwal 23955–6900, Kingdom of Saudi Arabia.
*Present address: Vilcek Institute of Graduate Biomedical Sciences, NYU Langone Health, New York, NY 10010, USA. ‡Present address: Genetics and Epigenetics Program, The University of Pennsylvania, Philadelphia, PA 19104, USA. §Present address: University of Pennsylvania, Philadelphia, PA 19104, USA.
¶These authors contributed equally to this work

**Author for correspondence (sam.gu@rutgers.edu)

S.G., 0000-0002-5861-3630

Handling Editor: Swathi Arur
Received 28 February 2022; Accepted 14 July 2022

Development (2022) 149, dev200692. doi:10.1242/dev.200692

Despite the clear distinctions in their abundance and biochemical properties, how cells distinguish the self and nonself siRNAs remains largely unknown. Transposons and self genes differ significantly in their chromatin environment, modes of transcription, RNA processing and trafficking, which can all potentially affect siRNA production and loading into AGOs. However, it is hard to change one factor without affecting other, which makes it difficult to interpret the results obtained from using mutants in the aforementioned pathways. In this study, we took a genome engineering approach to insert various self-gene and *gfp* DNA fragments into an LTR retrotransposon *Cer3*, which is a natural 'hot spot' of nonself siRNAs. This enabled us to examine the propensity of self-gene fragments in producing siRNAs when embedded in a nonself siRNA-producing genomic environment.

RESULTS

The design of ectopic siRNA production from the LTR retrotransposon *Cer3*

In this study we used CRISPR to insert ∼400 nt exonic sequences from various protein-coding genes into the LTR retrotransposon *Cer3* to test whether the protein coding gene fragments produce ectopic siRNAs (Fig. 1A). *Cer3* is a native target of germline nuclear RNAi and produces abundant germline-specific siRNAs (Fig. 1B; Figs S1A, S2) (Ni et al., 2014, 2018). There is only one copy of *Cer3* in the genome of the wild-type (WT) Bristol N2 strain. The insertion site was chosen for its local peak level of siRNA production (Fig. S2). Single nucleotide polymorphisms (SNPs) were introduced in some of the insertions at 30 nt intervals to distinguish between the transposon-driven ectopic siRNAs and the native self siRNAs (generated from the homologous target genes).

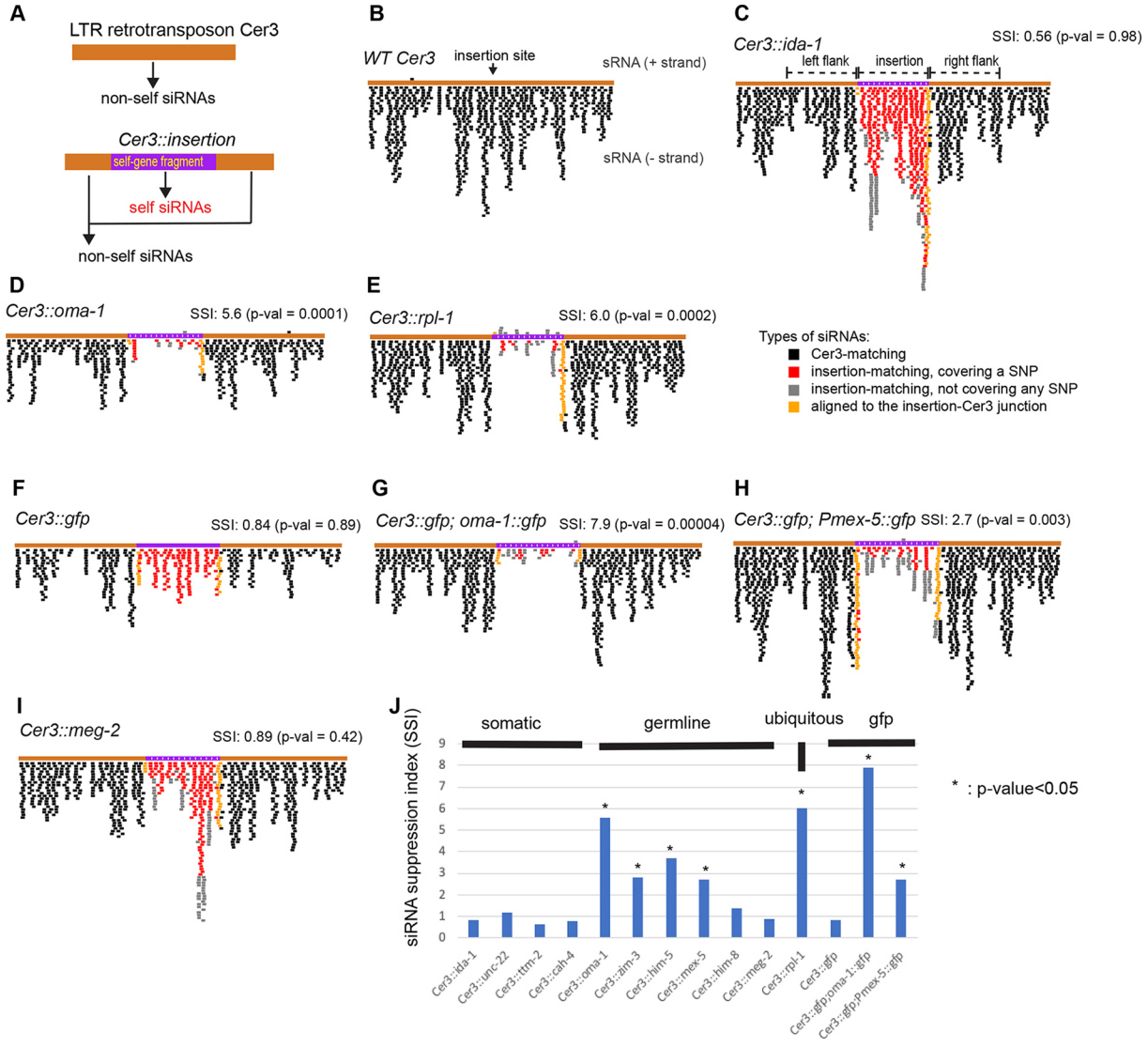

Fig. 1. Differential expression of ectopic self siRNAs driven by LTR retrotransposon *Cer3*. (A) Schematic of *Cer3* with a CRISPR-engineered insertion (*Cer3::insertion*) to express ectopic siRNAs. (B-I) siRNA track plots for WT *Cer3* and various *Cer3::insertion* alleles. Only the insertion and the 1.4 kb *Cer3* sequence (700 bp on either side of the insertion) are included in the plots. Individual sense and antisense small RNA reads with perfect alignment to the *Cer3::insertion* sequences are plotted above and below the gene track, respectively. siRNA tracks are color-coded to reflect their locations as indicated in the legend. Additional *Cer3::insertion* siRNA track plots are in Fig. S4. The siRNA suppression index (SSI=*Cer3* siRNA density of the 400 bp left and right flanking sequences/siRNA density of the insertion) and *P*-value are indicated for each panel. (J) Bar graph of siRNA suppression indexes for various *Cer3* alleles shown in Fig. 1 and Fig. S4. The *P*-values were calculated using Wilcoxon Rank Sum test with the null hypothesis that the density of siRNAs mapped to the insertion is the same or larger than the density of flanking *Cer3* siRNAs.

Development (2022) 149, dev200692. doi:10.1242/dev.200692

Suppression of *Cer3*-driven ectopic siRNAs against germline genes

Synchronized young adults carrying various *Cer3::insertion* mutations were the subject of small RNA-sequencing (sRNA-seq) analysis. We found that none of the insertions used in this study affected *Cer3* siRNA expression (Fig. 1; Fig. S3). However, the levels of ectopic siRNAs from different insertions varied significantly. Insertions of a *gfp* fragment (*Cer3::gfp*) (Fig. 1F) and four somatic gene fragments [*ida-1*, *ttm-2*, *cah-4* and *unc-22*, selected for preferentially neuronal, intestinal, hypodermal or muscle expression, respectively, based on RNA-seq data from Serizay et al. (2020)] (Fig. 1C; Fig. S4A-C) produced abundant siRNAs, with levels similar to the ones expressed from the flanking *Cer3* sequences (Fig. 1J). In contrast, fragments from four germline-expressed genes (*oma-1*, *zim-3*, *him-5* and *mex-5*) and one ubiquitously expressed ribosomal protein gene (*rpl-1*) produced significantly fewer siRNAs than the flanking *Cer3* siRNAs (Fig. 1D,E,J; Fig. S4D-E,G). We also crossed the *Cer3:gfp* allele into strains that carry a germline-expressed *gfp* transgene, either a translational fusion of *oma-1::gfp* or *gfp* driven by a germline-specific promoter (*Pmex-5::oma-1*). We found that the *Cer3*-driven *gfp* siRNAs were produced in much lower abundance in both the *gfp* transgene (+) animals than in the *gfp* transgene (−) animals (Fig. 1G,H). In total, we tested nine strains in which germline-expressed fragments were inserted into *Cer3*. Although most of the *Cer3::insertion*-containing germline gene fragments exhibited suppressed level of siRNAs produced from the insertions (Fig. 1D,E,G,H; Fig. S4D-G), we did observed two exceptions from the *Cer3::meg-2* (Fig. 1I) and *Cer3::him-8* (Fig. S4F), which produced abundant siRNAs from the insertions. We do not know the reason for these exceptions at this point (some speculations are given in the Discussion).

To compare the relative expression of siRNAs from *Cer3* and insertions, we defined an siRNA suppression index (SSI) as the ratio between the density of flanking *Cer3* siRNAs and insertion siRNAs. The average SSI for the germline-expressed fragments (except *him-8* and *meg-2*) was 4.5. In contrast, the average SSI for *gfp* (WT background) and somatic fragments is 0.8. We also inserted the *oma-1* fragment into a different LTR retrotransposon, *Cer8*, and observed a similar suppressive effect on the production of the ectopic *oma-1* siRNAs (Fig. S4H,I). These results indicate that germline-expressed gene fragments tend to be protected from siRNA production even when embedded in siRNA hotspots such as in transposon sequences. We refer to this phenomenon as 'siRNA suppression' in this paper. The germline gene *oma-1* has been extensively used as a native gene to study RNAi and transgenerational epigenetic silencing (Alcazar et al., 2008). For the rest of the study, we used the *Cer3::oma-1* allele to characterize siRNA suppression.

The siRNA suppression effect is local and limited to the homologous sequence

We found that siRNA suppression did not spread to either side of the flanking *Cer3* sequences (Fig. 1B,D,G,H; Fig. S3A,C), suggesting that the siRNA suppression effect is local. To further test the local effect, we reduced the length of the sequence homology by deleting a 240 bp segment from the *oma-1* gene in the strain that carried the same *Cer3::oma-1* allele as used in Fig. 1D. The deleted sequence matches fragment B of *Cer3::oma-1* as indicated in Fig. 2A, leaving fragment A as the only sequence in *Cer3::oma-1* with homology to the mutant *oma-1*. We found that the *oma-1* deletion abrogated the siRNA suppression for fragment B, but not for fragment A (Fig. 2A). This result confirms that siRNA suppression requires the homologous DNA sequence in the target gene and that the suppression is highly local and does not spread to flanking non-homologous sequences in *Cer3*.

siRNA suppression is likely mediated by mRNA

We hypothesized that siRNA suppression is mediated by the target mRNA and thus tested the requirement of promoter, strand specificity, and the effect of mRNA silencing on siRNA suppression.

One way to abolish *oma-1* transcription is to delete the *oma-1* promoter. Our attempt on this using CRISPR was unsuccessful, so we used the available *oma-1[tm1396]* allele (*C. elegans* Deletion Mutant Consortium, 2012), which deletes a 1.5 kb sequence including the promoter and a large fraction of the transcribed sequence of *oma-1*, including part (232 bp) of the homologous sequence to *Cer3::oma-1* (Fig. 2B). In the remaining *oma-1* sequence, 187 bp still shared sequence homology to *Cer3::oma-1* (fragment C in Fig. 2B). We found that this *oma-1* mutation abrogated the siRNA suppression effect for the entire *oma-1* insertion of *Cer3::oma-1*, including fragment C (Fig. 2B), suggesting that the *oma-1* promoter is required for siRNA suppression.

To test the strand specificity, we compared two *Cer3::oma-1* alleles that differ in the orientation of the *oma-1* insertion, with one producing antisense *oma-1* siRNAs (Fig. 1D) and the other sense *oma-1* siRNAs (Fig. 2C). We found that, unlike the antisense *oma-1* siRNAs, sense *oma-1* siRNAs were not suppressed (Fig. 2C). Therefore, the siRNA suppression effect is specific to antisense siRNAs.

To test the effect of *oma-1* mRNA silencing on siRNA suppression, we first performed *oma-1* RNAi by feeding worms with dsRNA that targets a sequence upstream to the homologous sequence to *Cer3::oma-1* (Fig. S5A). We found that the siRNA suppression was not affected (Fig. S5A). We then performed a piRNA-triggered *oma-1* silencing (piRNAi) using a piRNA-expressing transgene approach recently developed by Priyadarshini et al. (2022). The target sites of the six artificial piRNAs spread along the *oma-1* gene (Fig. S6A). Consistent with the previous report (Priyadarshini et al., 2022), our RNA-seq analysis indicated that piRNAi induced a much more robust *oma-1* silencing (29.1-fold) than dsRNA (4.6-fold) (Fig. S5B,C). Two piRNA sites also fell into the *oma-1* sequence in *Cer3::oma-1* (Fig. S6A), and therefore may directly impact siRNA production from *Cer3::oma-1*. To rule out this possibility, we also generated a new *Cer3::oma-1* allele (red118) that deleted the two piRNA sites, but otherwise was identical to the allele (red20) that was frequently used in this study (Fig. S6A). We found that *oma-1* piRNAi abrogated the siRNA suppression for both alleles of *Cer3::oma-1* (Fig. 2D; Fig. S6A), whereas the control samples of *unc-119* piRNAi (Fig. 2E) or no piRNAi (Fig. S6B) exhibited strong siRNA suppression at *Cer3::oma-1*. These results suggest that siRNA suppression can be reversed by a strong silencing of the target gene (by piRNAi). Because siRNA suppression is not affected by a more modest silencing effect of the target gene (by dsRNA), we suggest that the amount of mRNA needed for siRNA suppression can be low.

Taken together, these results strongly suggest that siRNA suppression is mediated by the mRNA of the homologous germline gene.

siRNA suppression does not require the germline AGO proteins HRDE-1 and CSR-1 or the piRNA pathway, but it does require the P-granule components

We then performed a small scale candidate gene-based screen to investigate the genetic requirement of siRNA suppression using *Cer3::oma-1*. CSR-1 and HRDE-1 are two germline-specific AGO

Development (2022) 149, dev200692. doi:10.1242/dev.200692

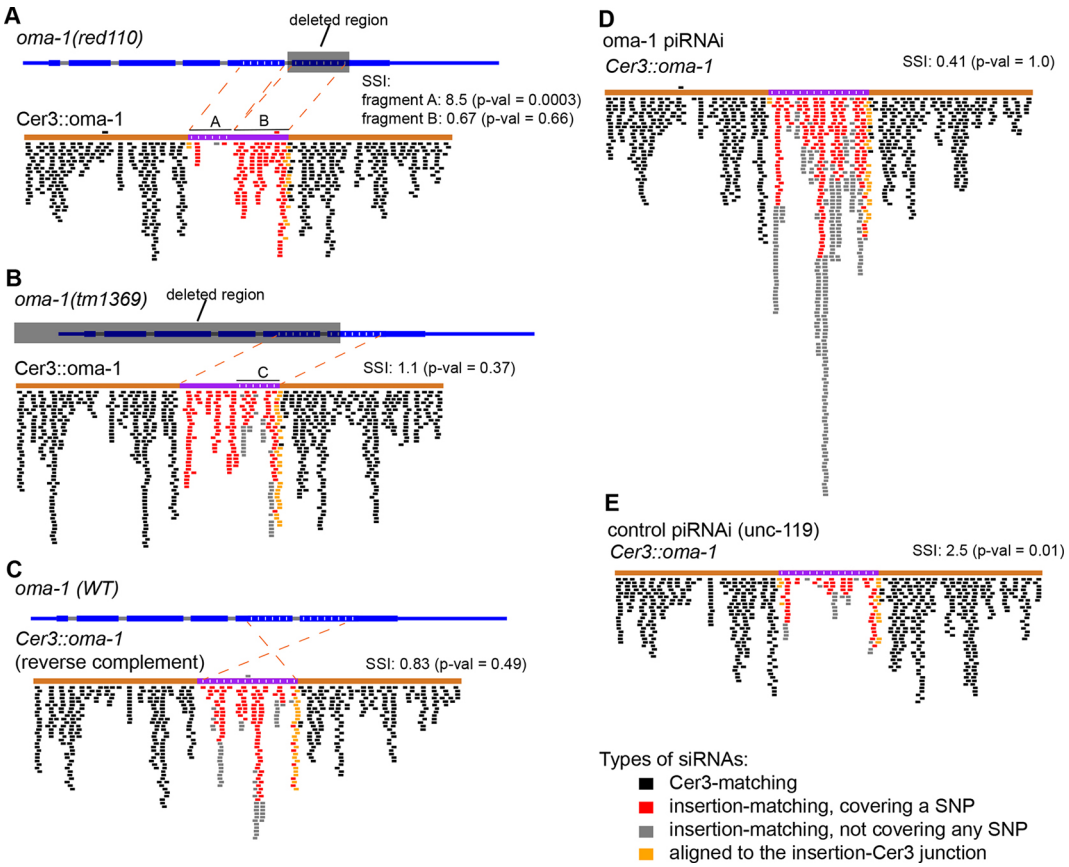

Fig. 2. siRNA suppression requires mRNA expression of the homologous gene. (A,B) *Cer3::oma-1* siRNA track plots for strains carrying *oma-1* deletion mutations (A: *red110*; B: *tm1396*). Deleted regions are indicated by transparent gray boxes. (C) siRNA track plot for *Cer3::oma-1* that expresses sense-stranded *oma-1* siRNAs. (D,E) siRNA track plots for *Cer3::oma-1* in *oma-1* piRNAi animals and in control animals (*unc-119* piRNAi). See Fig. S5 for mRNA-seq results of piRNAi-induced *oma-1* mRNA silencing and Fig. S6 for additional experiments of *oma-1* piRNAi.

proteins that preferentially bind different populations of germline siRNAs: self siRNAs for CSR-1 and nonself siRNAs for HRDE-1 (Claycomb et al., 2009; Ashe et al., 2012; Buckley et al., 2012; Shirayama et al., 2012). We found that neither the *hrde-1*(−) mutation nor CSR-1 depletion by auxin-induced protein degradation (AID) affected the siRNA suppression of *Cer3::oma-1* (Fig. 3A-C,I; Fig. S7), indicating that HRDE-1 and CSR-1 are not required for siRNA suppression in adult animals. In our experiment, CSR-1 depletion occurred continuously from the embryo to the adult stage. Consistent with the published work (Claycomb et al., 2009), CSR-1 depletion caused a complete embryonic lethal phenotype (data not shown), which prevented us from examining any intra- or intergenerational impact on siRNA suppression. Therefore, we cannot rule out the possibility that CSR-1 promotes the establishment of siRNA suppression either in the early embryo or in the previous generation but is not required for the maintenance of siRNA suppression in adults.

Recent studies have shown that the piRNA pathway can suppress the runaway siRNA amplification in *C. elegans* (Shukla et al., 2020; Montgomery et al., 2021; Wahba et al., 2021). The PRDE-1 protein is required for the biogenesis of piRNAs (Kasper et al., 2014; Weick et al., 2014) and PRG-1 is the PIWI protein that binds piRNAs (Batista et al., 2008); both are essential for piRNA-mediated functions (Billi et al., 2014). We observed strong siRNA suppression of *Cer3::oma-1* in the *prg-1*(−) and *prde-1*(−) animals (Fig. 3D,E,I), indicating that piRNA activity is not required for siRNA suppression of *Cer3::oma-1*.

The P granules in *C. elegans* germline are liquid-like membraneless condensates of RNA and proteins that often locate adjacent to the cytoplasmic side of the nuclear pore complexes (Strome and Wood, 1982). Many proteins in the RNAi pathway are enriched in the P granules, and the P granules have been shown to promote RNAi (Seydoux, 2018; Marnik and Updike, 2019). Consistent with this notion, we found that mutant animals lacking any of the P-granule assembly factors DEPS-1, GLH-1 and PGL-1 showed reduced levels of *Cer3* siRNAs (Fig. S8). We crossed the *Cer3::oma-1* allele into these P-granule mutants. We sequenced deeper for these samples in order to obtain sufficient siRNA reads to quantify siRNA suppression at *Cer3::oma-1*. We found that the siRNA suppression effect was abrogated in *deps-1*(−) and *glh-1*(−) animals (Fig. 3F,G). The *pgl-1*(−) mutation also weakened the siRNA suppression effect, albeit to a lesser degree than *deps-1*(−) or *glh-1*(−) (Fig. 3H). These results suggest that siRNA suppression requires functional P granules.

Unsuppressed ectopic siRNAs induce transitive RNAi of the target gene

To determine the impact of *Cer3*-driven ectopic siRNAs on the target gene mRNA expression, we performed RT-qPCR analyses of the corresponding target genes in worms carrying the *Cer3::oma-1*, *Cer3::zim-3*, *Cer3::rpl-1* or *Cer3::meg-2* alleles. For the *Cer3::oma-1*, *Cer3::zim-3* and *Cer3::rpl-1* alleles, which all exhibited strong siRNA suppression, their corresponding target gene mRNAs were expressed at the WT level (Fig. 4A-C), and their overall siRNA

Development (2022) 149, dev200692. doi:10.1242/dev.200692

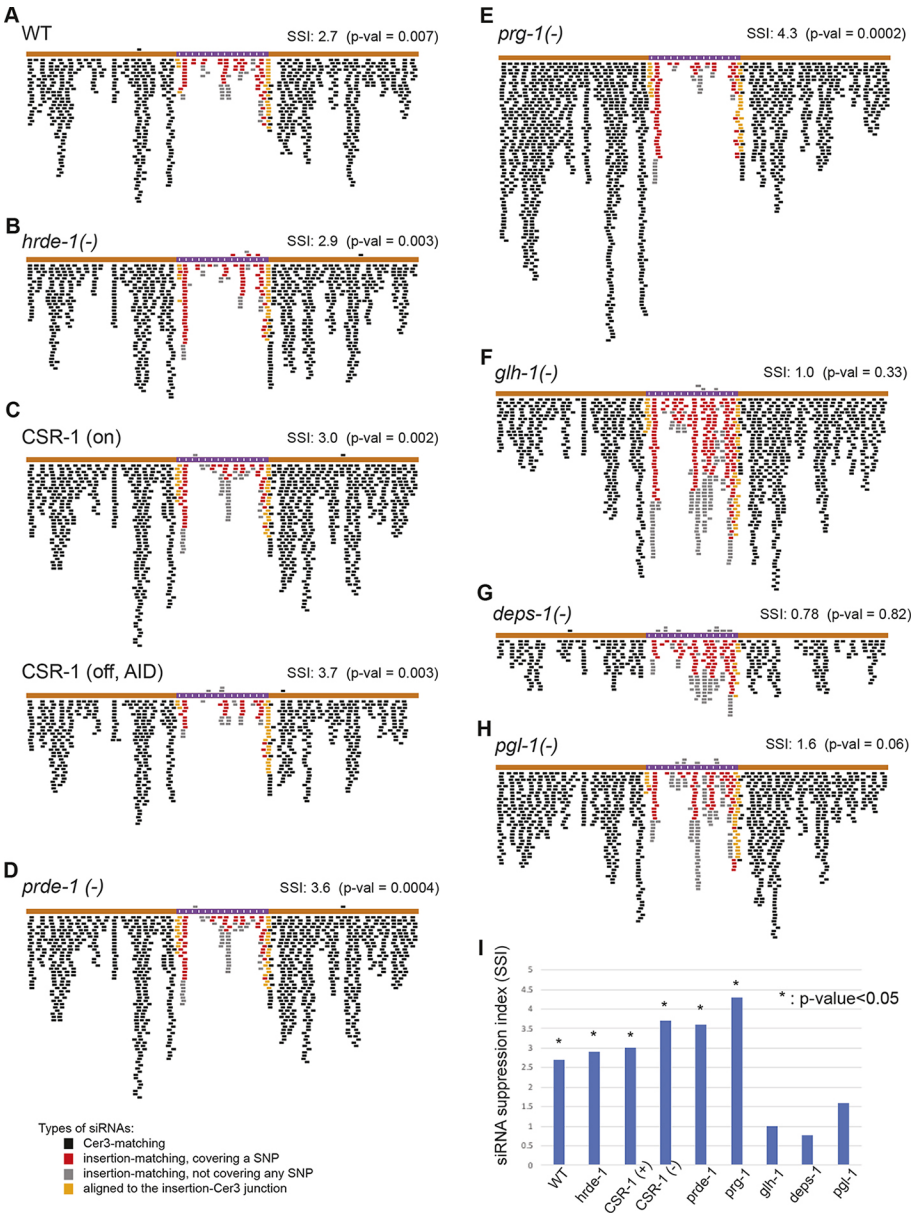

Fig. 3. Genetic requirement of siRNA suppression of *Cer3::oma-1*. (A,B,D-H) *Cer3::oma-1* siRNA track plots for WT animals and various loss-of-function mutants as indicated in each panel. (C) *Cer3::oma-1* siRNA track plots for animals with auxin-induced degradation (AID) of CSR-1 (lower panel) and control animals (upper panel). See Fig. S7 for the CSR-1 western blotting result. (I) Bar graph of siRNA suppression indexes (SSIs) for the experiments shown in panels A-H. A Wilcoxon Rank Sum test was used to calculate the *P*-values (see Materials and Methods).

levels, as well as the relative siRNA distribution along the gene body, were not affected (Fig. 4E-G,I-K), indicating a lack of RNAi at these genes. In contrast, *Cer3::meg-2*, which is resistant to siRNA suppression, was associated with a 43% reduction in *meg-2* mRNA (Fig. 4D) and a 28-fold increase in *meg-2* siRNAs (Fig. 4H), with the most prominent siRNA increase at the region homologous to the inserted sequence in *Cer3::meg-2* (Fig. 4L). These results indicate that the *Cer3*-driven ectopic siRNAs, if not suppressed, can induce a transitive RNAi effect at the target gene.

siRNA suppression of the native siRNAs

So far, our experiments only examined ectopic siRNAs expressed from genetically engineered loci. We next wished to determine whether the native nonself siRNA can be suppressed by an increased level of homologous mRNA. We took two different approaches to increase the level of the homologous mRNA.

First, we inserted a 467 nt *Cer3* fragment in the 3′ untranslated region (UTR) of the native *oma-1* gene (*oma-1::Cer3*) (Fig. 5A) and examined its impact on siRNA expressions of *oma-1* and *Cer3*. The *Cer3* fragment was chosen for its high siRNA expression in *Cer3*. Although the *Cer3* insertion produced more siRNAs than the flanking *oma-1* sequence (Fig. S9A), it did not significantly affect the expressions of *oma-1* mRNA or siRNA (Fig. S9B,C). However, the *oma-1::Cer3* mutant animals exhibited a striking suppression of siRNA production in *Cer3*. Like the cases mentioned earlier, the siRNA suppression effect was specific to the homologous sequence without spreading to the adjacent *Cer3* sequence (Fig. 5A,B; Fig. S9D).

In our second experiment, we asked whether *hrde-1* mutation can lead to siRNA suppression at the desilenced native HRDE-1 targets. To this end, we analyzed our previously published mRNA-seq and sRNA-seq data of the WT and *hrde-1*(−) animals cultured at 23°C (Ni et al., 2016). Out of the top 20 desilenced genes in the *hrde-1*(−) mutant (>16-fold desilencing, $P<0.05$) (Fig. 5C), 12 genes had at least threefold decreases in siRNA expression ($P<0.05$) (Fig. 5D). Such association supports the idea that desilencing of the native HRDE-1 targets leads to suppression of siRNA production. However, certain AGO proteins (e.g. PRG-1; Batista et al., 2008)

Development (2022) 149, dev200692. doi:10.1242/dev.200692

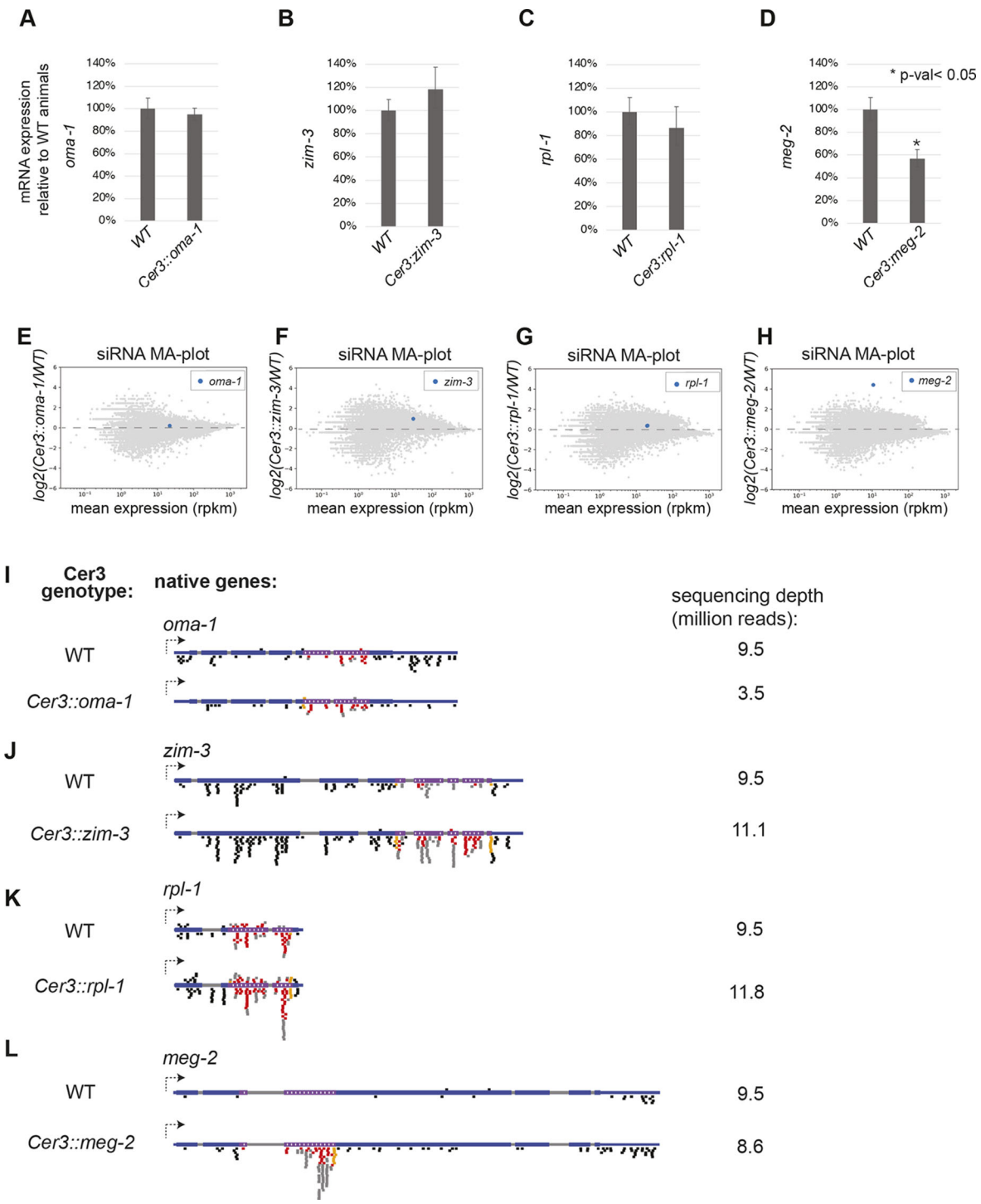

Fig. 4. The impact of *Cer3*-driven ectopic siRNAs on target gene mRNA and siRNA expression. (A-D) RT-qPCR analysis of the corresponding target gene mRNA for WT and *Cer3* mutant animals. Data are mean+s.d. *P*-values were calculated using a paired two-tailed Student's *t*-test. (E-H) sRNA-seq analysis [MA (log-ratio versus mean average)-plots] comparing WT and a *Cer3* mutant strain for all genes. The corresponding target gene in each panel is highlighted. (I-L) siRNA track plots for corresponding target genes of the ectopic siRNAs expressed from the *Cer3::insertion* alleles (the bottom plot in each panel). The top plot in each panel shows the sRNA profile of the same gene in WT *Cer3* animals. The region homologous to the *Cer3::insertion* was colored in purple, with SNPs indicated in vertical lines. SNP matching reads are in red. Reads that are in between two adjacent SNPs are in gray. Reads covering the junctions of the homologous sequence and the flanking sequence are in orange. Arrows indicate the gene transcription direction.

have been shown to promote the stability of the bound small RNAs. For this reason, we also examined the *nrde-2* mutant. NRDE-2 is an effector nuclear RNAi factor, functioning downstream of the siRNA production, and itself is not an AGO protein (Guang et al., 2010). Therefore, the loss of NRDE-2 is unlikely to have any direct impact on the siRNA biogenesis or turnover. Similar to *hrde-1*, *nrde-2* mutation also caused losses of siRNAs at the desilenced native HRDE-1 targets (Fig. 5E-G), which further supports that desilencing of the native HRDE-1 targets can suppress the production of the targeting siRNAs.

Development (2022) 149, dev200692. doi:10.1242/dev.200692

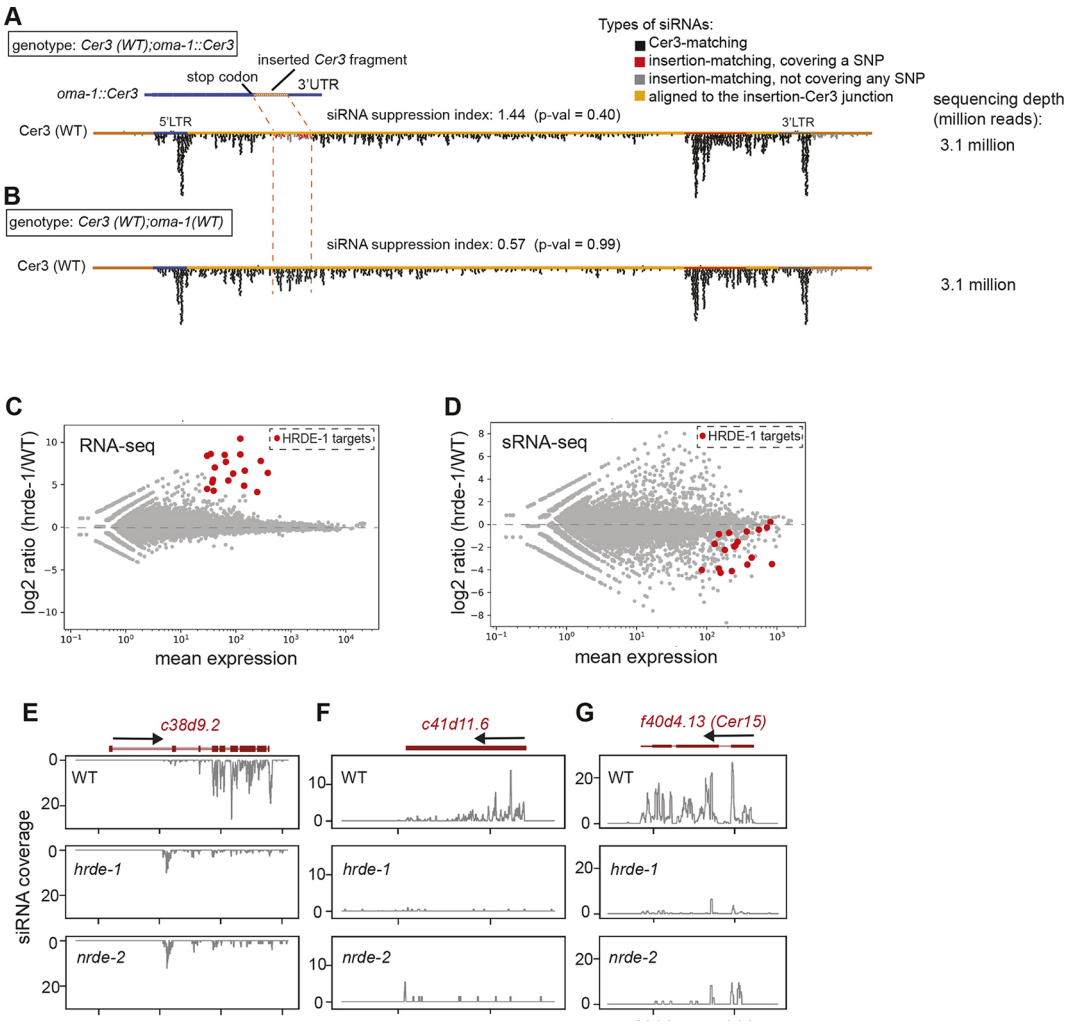

Fig. 5. Suppression of native nonself siRNAs. (A) siRNA track plot of a full-length WT *Cer3* in the *oma-1::Cer3* mutant, in which a 467 nt *Cer3* sequence was inserted immediately after the stop codon of *oma-1*, with SNPs every 30 nt. (B) *Cer3* siRNA track plot for WT animals. The same number of total small RNA reads were used for A and B. A normalized *Cer3* siRNA coverage plot of the same libraries used in A and B is shown in Fig. S9D. A Wilcoxon Rank Sum test was used to calculate the *P*-values (see Materials and Methods). (C,D) MA (log2 ratio versus mean average)-plots comparing *hrde-1* and WT RNA-seq (C) and sRNA-seq (D). Top 20 HRDE-1 target genes were highlighted in red. (E-G) sRNA coverage plots for three different HRDE-1 targets in WT, *hrde-1* and *nrde-2* mutants, as indicated.

Taken together, these results indicate that siRNA suppression is not limited to genetically engineered ectopic siRNAs, but can also occur to native siRNAs when the homologous mRNA sequence is actively expressed *in cis* or *in trans*.

Cer3-driven ectopic siRNAs are preferentially loaded in HRDE-1 over CSR-1

As mentioned earlier, HRDE-1 prefers to bind nonself siRNAs and CSR-1 prefers to bind self siRNAs. We wanted to determine whether the *Cer3*-driven ectopic siRNAs are preferentially loaded into HRDE-1 or CSR-1. To this end, we generated a strain that expresses *Cer3::oma-1*, SF(strep II-FLAG)-HRDE-1 and c-myc-CSR-1 and sequenced the HRDE-1-bound siRNAs and CSR-1-bound siRNAs using the small RNA co-immunoprecipitation (sRIP)-seq experiment. The relative HRDE-1 or CSR-1 preference was measured by the ratio of sRIP-seq signal (HRDE-1 or CSR-1 IP, respectively) over the input signal. We first confirmed that siRNAs from known HRDE-1 targets, such as *Cer3*, *bath-45* and *f15d4.5*, were much more enriched in the HRDE-1 co-immunoprecipitation siRNAs than in the CSR-1 ones (Fig. 6). In contrast, germline genes such as *oma-1*, *prg-1* and *pgl-1* showed higher relative enrichment in CSR-1 than in HRDE-1 (Fig. 6), as expected. Similar to the *Cer3* siRNAs, the ectopic *oma-1* siRNAs from *Cer3::oma-1* showed a much higher enrichment in HRDE-1 than in CSR-1 (Fig. 6), indicating a strong preference of HRDE-1 over CSR-1 for *Cer3*-driven ectopic siRNAs.

DISCUSSION

One paradox of RNAi is that the mRNAs are both the target and a necessary component of RNAi, as mRNAs are the substrates or templates for siRNA biogenesis. Here, we show that the target transcripts can also suppress the homologous siRNAs. This further increases the complexity in the mRNA-siRNA relationship and epigenetic regulation in *C. elegans* germline (Fig. 7). We suggest that nonself DNA, such as transposons, are active in producing endo-siRNAs but inactive in siRNA suppression due to the low level of their mRNAs. The germline-expressed genes (self DNA) are the opposite: relatively low activity in siRNA biogenesis but high activity in siRNA suppression due to the high level of mRNAs. Previous studies have shown that factors that promote siRNA

Development (2022) 149, dev200692. doi:10.1242/dev.200692

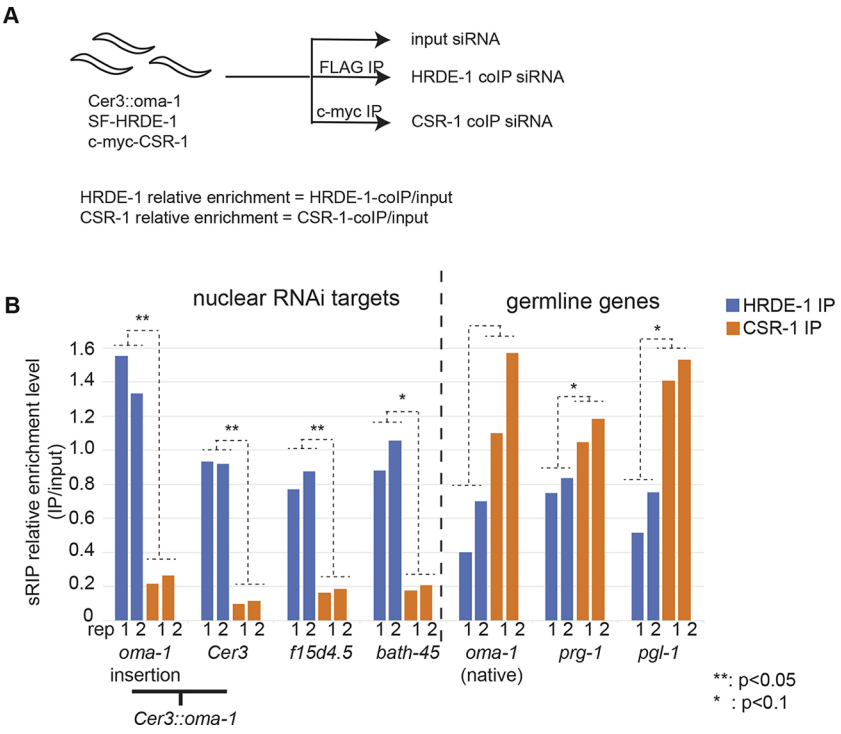

Fig. 6. *Cer3*-driven ectopic siRNAs are preferentially loaded in HRDE-1 over CSR-1. (A) Schematic of the HRDE-1 and CSR-1 (small RNA CoIP) sRIP-seq experiment. (B) HRDE-1 and CSR-1 sRIP relative enrichment levels for various genes. Two biological replicates were individually plotted. For *oma-1* insertion of *Cer3::oma-1*, only SNP-containing reads were considered. For *Cer3*, only the 400 nt flanking region on each side of the *oma-1* insertion was used. For the native *oma-1* gene, the *Cer3::oma-1* homologous sequence was excluded from the analysis because *Cer3::oma-1* caused a moderate increase in siRNA levels at this region (data not shown). The full-length cDNA sequences were used for other genes in this panel. A paired two-tailed Student's *t*-test was used to calculate the *P*-values in R.

turnover play a key role in preventing unwanted silencing in the genome (van Wolfswinkel et al., 2009; Pisacane and Halic, 2017; Zhou et al., 2017; Wang et al., 2020). In these cases, it was unclear to what extent the siRNA turnover was dependent on the target mRNA. Our study demonstrates that target-dependent suppression of siRNA production is an integral component of the RNAi pathway in *C. elegans* germline and plays an important role in distinguishing self and nonself genetic material.

Potential biological functions

RNAi in *C. elegans* germline is highly robust and long-lasting (Fire et al., 1998; Grishok et al., 2000; Vastenhouw et al., 2006; Alcazar et al., 2008; Devanapally et al., 2021). These features, although essential for genome surveillance against nonself DNA, can potentially lead to unwanted silencing of self genes. Previous studies have shown that epimutations of self genes can be induced by a diverse set of experimental triggers and genetic conditions (Johnson and Spence, 2011; Ashe et al., 2012; de Albuquerque et al., 2015; Phillips et al., 2015; Shukla et al., 2020; Montgomery et al., 2021; Wahba et al., 2021). The risk of epimutation is further increased by the presence of the siRNAs that are naturally produced from germline genes. For example, rRNA genes appear to be particularly prone to aberrant siRNA production and silencing (Zhou et al., 2017; Reed et al., 2020; Montgomery et al., 2021; Wahba et al., 2021). Some active genes contain siRNA-producing transposon elements in their introns or nearby intergenic regions. In addition, a recent epimutation accumulation study found that siRNAs can increase for certain self-genes in WT populations (Beltran et al., 2020). Interestingly, such increases appear to be transient. These observations highlight the importance of regulating self-targeting siRNAs.

The aberrant RNAi of self genes is likely to be prevented by multiple mechanisms. The lack of silencing triggers, such as dsRNA, piRNA, 26G-RNA, pUG or other untemplated tails, is likely the major reason for the absence or low level of siRNAs from self genes (Billi et al., 2014). The target-dependent siRNA suppression can provide another mechanism against unwanted silencing by distinguishing the self and nonself siRNAs. Given the

Fig. 7. A model of the complex interactions between mRNAs and siRNAs. (1) mRNAs are the target of siRNAs for RNAi; (2) mRNAs are needed for siRNA biogenesis; (3) mRNAs can also suppress siRNA production. Nonself genes are active in siRNA biogenesis and RNAi, and inactive in siRNA suppression, likely owing to the low level of mRNAs. Self genes are active in siRNA suppression likely owing to the high level of mRNAs, which at least partially prevents self genes from runaway siRNA amplification and aberrant RNAi activity.

Development (2022) 149, dev200692. doi:10.1242/dev.200692

large difference in the mRNA levels between self and nonself genes, the dependence on the target mRNA can ensure the specificity of self-siRNA suppression and avoid suppression of the nonself siRNAs. Target-directed siRNA suppression may also contribute to the previously observed non-coding function of mRNA in promoting gene expression (Johnson and Spence, 2011; Seth et al., 2013, 2018; Devanapally et al., 2021). We note that target-directed siRNA suppression did not completely abolish ectopic siRNAs. Rather, this feature is perhaps important for fine tuning the siRNA levels of germline genes.

Mechanistic considerations

siRNA synthesis or degradation?

In principle, there are two ways to achieve target-directed siRNA suppression: inhibiting siRNA biogenesis or enhancing siRNA turnover. At this point we find it difficult to imagine how target mRNAs directly inhibit ectopic siRNA synthesis. siRNAs produced from the target mRNA, on the other hand, can potentially bind to the homologous RNA sequence inserted in *Cer3* and function as a barrier against the RdRP activity, as suggested by Shen et al. (2018). However, such a model would predict that the *Cer3* siRNAs that are immediately upstream of the insertion would be suppressed as well. We did not observe such an effect. Instead, the siRNA suppression was highly limited to the homologous sequence. Although we cannot rule out a model involving siRNA synthesis inhibition, we currently favor a target mRNA-mediated siRNA degradation model, perhaps using a mechanism that is similar to target-dependent microRNA degradation (Ameres et al., 2010; Sheu-Gruttadauria et al., 2019) or RNA tailing-mediated sRNA degradation (van Wolfswinkel et al., 2009; Pisacane and Halic, 2017; Zhou et al., 2017; Wang et al., 2020; Yang et al., 2020). In addition, the steady state level of siRNAs can also be affected by activities that influence the ability of AGO proteins to bind siRNAs (Gudipati et al., 2021). We did not observe any above-background level of tailing for *Cer3*-driven ectopic siRNAs (data not shown), but we cannot rule out the possibility of rapid siRNA degradation after tailing. Recent studies have shown that the piRNA pathway, in addition to its silencing role, protects the rRNA locus, histones and other self genes from aberrant siRNA production and silencing (Shukla et al., 2020; Montgomery et al., 2021; Wahba et al., 2021; Priyadarshini et al., 2022). Future studies are needed to determine to what extent these activities are directed by target RNA.

P granules

We found that loss of P-granule components GLH-1, DEPS-1 or PGL-1 led to a defect in siRNA suppression. Future studies are needed to test whether siRNA suppression occurs in the P granules. Such a possibility is intriguing in that the P granules and other adjacent paranuclear condensates have been suggested as a hub for siRNA production and mRNA aggregation (Seydoux, 2018). The close proximity of siRNA biogenesis and siRNA suppression could reduce the chance of the unwanted siRNAs escaping from the quality control mechanism. One complication is that mutations in *glh-1*, *deps-1* and *pgl-1* also reduce endo-siRNA production at *Cer3* and elsewhere, which compromises the use of these mutants in studying the function of siRNA suppression.

The exceptions

Our study showed that germline expression of the target mRNA is a necessary factor but not a sufficient determinant in siRNA suppression. Additional factors can be chromatin marks, modes of transcriptional and post-transcriptional regulation, sub-cellular localization of mRNAs, and levels and AGO preference of endo-siRNAs. Future studies are needed to identify additional rules of siRNA suppression.

We suggest that the target-dependent suppression of siRNA production may distinguish self and nonself siRNA and play additional functions in other eukaryotes. We also note that such activity should be considered in mRNA-based technology and therapy.

MATERIALS AND METHODS

C. elegans culture

C. elegans were cultured at 20°C on nematode growth media (NGM) plates seeded with *Escherichia coli* OP50 as previously described (Brenner, 1974), unless indicated otherwise. Synchronized young adult animals, prepared as described in Ni et al. (2016), were used for all experiments in this study.

CRISPR

CRISPR experiments were conducted using previously described protocols (Arribere et al., 2014; Paix et al., 2015). Briefly, the injection mix generally consisted of 1 µg/µl Cas9 (IDT), 2.5 µM *dpy-10* sgRNA (Synthego), 0.4 µM ssDNA oligo as *dpy-10* [*cn64*] repair template, 10 µM target sgRNA, target repair template DNA [2 µM for ssDNA oligo or 0.4 µM for dsDNA with single-stranded overhangs generated using a method described by Dokshin et al., 2018)]. All CRISPR-generated mutations were confirmed by Sanger sequencing and are described in the supplementary Materials and Methods.

Design of the *Cer3*-based siRNA generator

An ∼400 nt cDNA sequence from *C. elegans* protein-coding genes or *gfp* was inserted into *Cer3* between base positions 914,783 and 914,784 of chromosome IV (WS190). Single-nucleotide mismatches separated by 30 nt intervals were introduced to the inserted sequence to distinguish siRNAs produced from the *Cer3::insertion* locus and ones from native genes.

Small RNA library preparation and sequencing

Small RNA extraction was performed using the MirVana kit (Thermo Fisher Scientific). Small RNA libraries were constructed using the 5′-monophosphate-independent, linker ligation-based method as described in Ni et al. (2016). A mixture of barcodes (set 1: AGCG, CGTC, GTTA and TATG; set 2: CTGG, ACTG, GAAG and TGCC) were added to the 5′ end of small RNA for each library, as indicated in the data deposited in the NCBI GEO database (GSE196847). The standard Illumina Hi-seq indexes (8 nt) were added at the PCR step to allow multiplexing. The libraries were pooled and sequenced on the Illumina HiSeq instrument. Library names and other information are listed in Table S1.

HRDE-1 and CSR-1 sRIP-seq

HRDE-1 and CSR-1 were endogenously tagged at their N-termini with the Strep-tag II-FLAG tag (DYKDDDDKGSAASWSHPQFEKGGGSG-GGSGGGSWSHPQFEK) (Ni et al., 2018; Gloeckner et al., 2009) and the c-myc tag (EQKLISEEDL), respectively. CSR-1 has two isoforms (F20D12.1a and F20D12.1b). The c-myc was tagged to the N-terminus of the shorter isoform F20D12.1b, which is constitutively expressed in the germline (Charlesworth et al., 2021). *Cer3::oma-1;sf-hrde-1;c-myc-csr-1* adult animals were used for the sRIP experiment. Cells were lysed by grinding the worms in liquid nitrogen with mortar and pestle.

HRDE-1 immunoprecipitation (IP) was performed using the FLAG Immunoprecipitation kit (Sigma-Aldrich, FLAGIPT1-1KT). Briefly, each worm grind (∼5000 young adults pulverized in liquid nitrogen) was lysed in 1 ml lysis buffer (Sigma-Aldrich, FLAGIPT1-1KT) with 10 µl of HALT protease inhibitor cocktail (Thermo Fisher Scientific) and 10 µl of RNAaseIn (Promega) at room temperature on a rotator for 15 min. Because HRDE-1 is a nuclear protein and might be chromatin bound, the crude lysate was sonicated using a Bioruptor (Diagenode) three times for 7.5 min at 4°C (setting: high, 30 s on and 30 s off). The lysis was clarified by centrifuging at 14,000 ***g*** for 4 min at 4°C and the lysis supernatant was collected and used

Development (2022) 149, dev200692. doi:10.1242/dev.200692

as IP input. The lysis supernatant was incubated with 40 µl of ANTI-FLAG M2 gel resin at 4°C overnight. And then the resin was washed three times in 1× Wash Buffer (Sigma-Aldrich, FLAGIPT1-1KT). The FLAG-tagged protein was eluted by competing with 150 µg/µl 3× FLAG peptide at 4°C for 30 min.

CSR-1 IP was performed using Pierce Magnetic c-Myc-Tag IP/CoIP kit (Thermo Fisher Scientific). Each worm grind (~5000 young adults pulverized in liquid nitrogen) was lysed in 1 ml Buffer-1 with 10 µl of HALT protease inhibitor cocktail (Thermo Fisher Scientific) and 10 µl of RNAaseIn (Promega) at room temperature on a rotator for 5 min. The lysis was clarified by spinning at 14,000 ***g*** for 10 min at 4°C. The lysis supernatant was used as IP input. The lysis supernatant was incubated with 25 µl of pre-washed anti-c-Myc magnetic beads at room temperature for 30 min. And then the beads were washed three times with 300 µl 1× Buffer-2. The c-Myc-tagged protein was eluted by 0.5 mg/ml c-Myc peptide in elution buffer at 37°C for 5 min. Western blotting was used to validate the HRDE-1 and CSR-1 IP (data not shown). The extract without any IP was used to prepare the Input small RNAs. Input and CoIP small RNAs were extracted using Phenol::$CHCl_3$ and sequenced as described in the previous section.

Bioinformatic analysis

To extract the small RNA reads, we first trimmed the 3′ linker sequence from the raw Illumina reads. We added a set of four 4 nt barcodes at the 5′ end of small RNAs for each library. We collapsed identical small RNA reads with identical barcodes to minimize bottlenecking caused by PCR amplification (identical small RNA reads with different barcodes were not collapsed). All sequence alignments were performed using Bowtie version 1.2.3 (Langmead et al., 2009). The 5′ barcodes were trimmed at the step of alignment. Only the 20-24 nt sRNA reads that perfectly aligned to the reference sequence were used for the analysis.

siRNA track plot, index calculation and statistics

Customized python scripts were used to make the siRNA track plots, in which individual sequenced sRNAs were drawn based on their alignment locations. Sense and antisense siRNAs were plotted separately above and below the gene track, respectively. Only perfectly aligned reads were used for the plots. When SNPs were used in the reference, reads were color coded as indicated in the figure legends. Briefly, a red track covers an SNP position and contains the SNP base used in the reference (therefore definitely derided from the SNP-containing reference). A gray track does not cover any SNP position, therefore can be derived from either the SNP-containing reference or the homologous target gene. Reads outside of the inserted sequence are colored in black. Reads covering the junctions of insertions are in orange. In some cases we also made the sRNA coverage plots (in R) by counting the number of sequenced reads at each base position, normalized by the sequencing depth (in millions).

The siRNA suppression index for insertions in *Cer3* was calculated as the ratio between antisense siRNA density in the 400 nt flanking sequences and the inserted sequence. Note that the ambiguous insertion siRNAs (ones that do not cover any SNP position) were included for the calculation. As some of the ambiguous siRNAs may come from the native gene, the true siRNA suppression index is likely to be higher than the calculated value.

To calculate the statistical significance of the siRNA suppression, we divided the insertion sequence and the 400 bp *Cer3* flanking sequences (left and right) into 50 nt bins. The number of siRNAs matching each bin were counted. The Wilcoxon Rank Sum test was performed for these two populations: counts for the insertion bins (G) and counts for the flanking bins (F), with the null hypothesis being G≥F.

Auxin-induced protein degradation of CSR-1

The degron-3×flag tag was added to the N-terminus of the longer isoform of CSR-1 (F20D12.1a) by CRISPR in the strain that carries the *Cer3::oma-1(red20)* and *sun-1p::TIR1::mRuby::sun-1* 3′ UTR (Zhang et al., 2015). Synchronized L1 larvae were cultured on plates containing 1 mM auxin or no auxin (as control) until reaching young adult stage, and were then harvested for sRNA-seq. CSR-1 AID was confirmed by both western blotting using the monoclonal anti-FLAG M2 antibody (Sigma-Aldrich, F1804-200UG, Lot: SLBG5673 V, 1:1000) (Fig. S7) and the sterility of auxin-treated animals (data not shown).

piRNA interference

oma-1 piRNAi was induced by an extrachromosomal array carrying the hygromycin-resistance gene and a cluster of piRNA expression units re-coded to target *oma-1* as described in Priyadarshini et al. (2022). The control *unc-119* piRNAi transgene was also the same as that used in Priyadarshini et al. (2022). The extrachromosomal array was selected by hygromycin resistance. The *oma-1* insertion used in the *Cer3::oma-1* (*red20*) allele contains two sites that can be targeted by piRNAs from the transgene. To rule out that the effect on siRNA suppression was due to interaction between *oma-1* piRNAs and *Cer3::oma-1*, we created a new *Cer3::oma-1* allele (*red118*) that deleted the two piRNA-target sites.

oma-1 mRNA expression analysis

oma-1 mRNA levels were measured using either RT-qPCR or RNA-seq as previously described (Kalinava et al., 2017). For RT-qPCR analysis, *oma-1* mRNA levels were normalized to *tba-1* mRNA levels. A paired two-tailed Student's *t*-test was used to calculate the *P*-values.

Acknowledgements

We thank Esteban Chen, Natallia Kalinava, Helen Ushakov and Elaine Gavin for technical assistance. We thank Andrew Fire for providing the python plotting program Very Simply Graphic (VSG). Some strains were provided by the *Caenorhabditis* Genetics Center, which is funded by NIH Office of Research Infrastructure Programs (P40 OD010440).

Competing interests

The authors declare no competing or financial interests.

Author contributions

Conceptualization: Z.G., D.K., J.N., S.G.; Methodology: Z.G., D.K., J.N., Z.Z., A.Z., M.G., M.K., J.H., M.P., C.F.-J., S.G.; Validation: D.K.; Formal analysis: Z.G., D.K., S.G.; Investigation: Z.G., D.K., J.N., Z.Z., A.Z., M.G., M.K., J.H., M.P., S.G.; Data curation: Z.G., D.K., S.G.; Writing - original draft: S.G.; Writing - review & editing: Z.G., D.K., C.F.-J., S.G.; Visualization: S.G.; Supervision: S.G.; Project administration: S.G.

Funding

Research reported in this publication was supported by the Busch Biomedical Grant from Rutgers, The State University of New Jersey, the National Institute of General Medical Sciences of the National Institutes of Health (R01GM111752 to S.G.) and by the King Abdullah University of Science and Technology Office of Sponsored Research (OSR-CRG2019-4016 to C.F.J.) Deposited in PMC for release after 12 months.

Data availability

Fastq files for the small RNA-sequencing results have been deposited in NCBI with the GEO accession number GSE196847.

References

Alcazar, R. M., Lin, R. and Fire, A. Z. (2008). Transmission dynamics of heritable silencing induced by double-stranded RNA in Caenorhabditis elegans. *Genetics* **180**, 1275-1288. doi:10.1534/genetics.108.089433

Ameres, S. L., Horwich, M. D., Hung, J. H., Xu, J., Ghildiyal, M., Weng, Z. and Zamore, P. D. (2010). Target RNA-directed trimming and tailing of small silencing RNAs. *Science* **328**, 1534-1539. doi:10.1126/science.1187058

Arribere, J. A., Bell, R. T., Fu, B. X., Artiles, K. L., Hartman, P. S. and Fire, A. Z. (2014). Efficient marker-free recovery of custom genetic modifications with CRISPR/Cas9 in Caenorhabditis elegans. *Genetics* **198**, 837-846. doi:10.1534/genetics.114.169730

Ashe, A., Sapetschnig, A., Weick, E. M., Mitchell, J., Bagijn, M. P., Cording, A. C., Doebley, A. L., Goldstein, L. D., Lehrbach, N. J., Le Pen, J. et al. (2012). piRNAs can trigger a multigenerational epigenetic memory in the germline of C. elegans. *Cell* **150**, 88-99. doi:10.1016/j.cell.2012.06.018

Batista, P. J., Ruby, J. G., Claycomb, J. M., Chiang, R., Fahlgren, N., Kasschau, K. D., Chaves, D. A., Gu, W., Vasale, J. J., Duan, S. et al. (2008). PRG-1 and 21U-RNAs interact to form the piRNA complex required for fertility in C. elegans. *Mol. Cell* **31**, 67-78. doi:10.1016/j.molcel.2008.06.002

Beltran, T., Shahrezaei, V., Katju, V. and Sarkies, P. (2020). Epimutations driven by small RNAs arise frequently but most have limited duration in Caenorhabditis elegans. *Nat. Ecol. Evol.* **4**, 1539-1548. doi:10.1038/s41559-020-01293-z

Billi, A. C., Fischer, S. E. and Kim, J. K. (2014). *Endogenous RNAi Pathways in C. elegans*, pp. 1-49. WormBook. doi:10.1895/wormbook.1.170.1

Brenner, S. (1974). The genetics of Caenorhabditis elegans. *Genetics* **77**, 71-94. doi:10.1093/genetics/77.1.71

Buckley, B. A., Burkhart, K. B., Gu, S. G., Spracklin, G., Kershner, A., Fritz, H., Kimble, J., Fire, A. and Kennedy, S. (2012). A nuclear Argonaute promotes multigenerational epigenetic inheritance and germline immortality. *Nature* **489**, 447-451. doi:10.1038/nature11352

Campbell, A. C. and Updike, D. L. (2015). CSR-1 and P granules suppress sperm-specific transcription in the C. elegans germline. *Development* **142**, 1745-1755. doi:10.1242/dev.121434

Cecere, G., Hoersch, S., O'Keeffe, S., Sachidanandam, , R. and Grishok, A. (2014). Global effects of the CSR-1 RNA interference pathway on the transcriptional landscape. *Nat. Struct. Mol. Biol.* **21**, 358-365. doi:10.1038/nsmb.2801

Charlesworth, A. G., Seroussi, U., Lehrbach, N. J., Renaud, M. S., Sundby, A. E., Molnar, R. I., Lao, R. X., Willis, A. R., Woock, J. R., Aber, M. J. et al. (2021). Two isoforms of the essential C. elegans Argonaute CSR-1 differentially regulate sperm and oocyte fertility. *Nucleic Acids Res.* **49**, 8836-8865. doi:10.1093/nar/gkab619

Claycomb, J. M., Batista, P. J., Pang, K. M., Gu, W., Vasale, J. J., van Wolfswinkel, J. C., Chaves, D. A., Shirayama, M., Mitani, S., Ketting, R. F. et al. (2009). The Argonaute CSR-1 and its 22G-RNA cofactors are required for holocentric chromosome segregation. *Cell* **139**, 123-134. doi:10.1016/j.cell.2009.09.014

C. elegans Deletion Mutant Consortium. (2012). Large-scale screening for targeted knockouts in the Caenorhabditis elegans genome. *G3* **2**, 1415-1425. doi:10.1534/g3.112.003830

de Albuquerque, B. F., Placentino, M. and Ketting, R. F. (2015). Maternal piRNAs are essential for germline development following De Novo establishment of Endo-siRNAs in caenorhabditis elegans. *Dev. Cell* **34**, 448-456. doi:10.1016/j.devcel.2015.07.010

Devanapally, S., Raman, P., Chey, M., Allgood, S., Ettefa, F., Diop, M., Lin, Y., Cho, Y. E. and Jose, A. M. (2021). Mating can initiate stable RNA silencing that overcomes epigenetic recovery. *Nat. Commun.* **12**, 4239. doi:10.1038/s41467-021-24053-4

Dokshin, G. A., Ghanta, K. S., Piscopo, K. M. and Mello, C. C. (2018). Robust genome editing with short single-stranded and long, partially single-stranded DNA donors in Caenorhabditis elegans. *Genetics* **210**, 781-787. doi:10.1534/genetics.118.301532

Fassnacht, C., Tocchini, C., Kumari, P., Gaidatzis, D., Stadler, M. B. and Ciosk, R. (2018). The CSR-1 endogenous RNAi pathway ensures accurate transcriptional reprogramming during the oocyte-to-embryo transition in Caenorhabditis elegans. *PLoS Genet.* **14**, e1007252. doi:10.1371/journal.pgen.1007252

Fire, A., Xu, S., Montgomery, M. K., Kostas, S. A., Driver, S. E. and Mello, C. C. (1998). Potent and specific genetic interference by double-stranded RNA in Caenorhabditis elegans. *Nature* **391**, 806-811. doi:10.1038/35888

Gent, J. I., Lamm, A. T., Pavelec, D. M., Maniar, J. M., Parameswaran, P., Tao, L., Kennedy, S. and Fire, A. Z. (2010). Distinct phases of siRNA synthesis in an endogenous RNAi pathway in C. elegans soma. *Mol. Cell* **37**, 679-689. doi:10.1016/j.molcel.2010.01.012

Gerson-Gurwitz, A., Wang, S., Sathe, S., Green, R., Yeo, G. W., Oegema, K. and Desai, A. (2016). A small RNA-catalytic argonaute pathway tunes germline transcript levels to ensure embryonic divisions. *Cell* **165**, 396-409. doi:10.1016/j.cell.2016.02.040

Gloeckner, C. J., Boldt, K. and Ueffing, M. (2009). Strep/FLAG tandem affinity purification (SF-TAP) to study protein interactions. *Curr. Protoc. Protein Sci.* **Chapter 19**, Unit19 20. doi:10.1002/0471140864.ps1920s57

Grishok, A., Tabara, H. and Mello, C. C. (2000). Genetic requirements for inheritance of RNAi in C. elegans. *Science* **287**, 2494-2497. doi:10.1126/science.287.5462.2494

Gu, W., Shirayama, M., Conte, D., Jr., Vasale, J., Batista, P. J., Claycomb, J. M., Moresco, J. J., Youngman, E. M., Keys, J., Stoltz, M. J. et al. (2009). Distinct argonaute-mediated 22G-RNA pathways direct genome surveillance in the C. elegans germline. *Mol. Cell* **36**, 231-244. doi:10.1016/j.molcel.2009.09.020

Guang, S., Bochner, A. F., Burkhart, K. B., Burton, N., Pavelec, D. M. and Kennedy, S. (2010). Small regulatory RNAs inhibit RNA polymerase II during the elongation phase of transcription. *Nature* **465**, 1097-1101. doi:10.1038/nature09095

Gudipati, R. K., Braun, K., Gypas, F., Hess, D., Schreier, J., Carl, S. H., Ketting, R. F. and Grosshans, H. (2021). Protease-mediated processing of Argonaute proteins controls small RNA association. *Mol. Cell* **81**, 2388-2402.e8. doi:10.1016/j.molcel.2021.03.029

Han, T., Manoharan, A. P., Harkins, T. T., Bouffard, P., Fitzpatrick, C., Chu, D. S., Thierry-Mieg, D., Thierry-Mieg, J. and Kim, J. K. (2009). 26G endo-siRNAs regulate spermatogenic and zygotic gene expression in Caenorhabditis elegans. *Proc. Natl. Acad. Sci. USA* **106**, 18674-18679. doi:10.1073/pnas.0906378106

Johnson, C. L. and Spence, A. M. (2011). Epigenetic licensing of germline gene expression by maternal RNA in C. elegans. *Science* **333**, 1311-1314. doi:10.1126/science.1208178

Kalinava, N., Ni, J. Z., Peterman, K., Chen, E. and Gu, S. G. (2017). Decoupling the downstream effects of germline nuclear RNAi reveals that H3K9me3 is dispensable for heritable RNAi and the maintenance of endogenous siRNA-mediated transcriptional silencing in Caenorhabditis elegans. *Epigenetics Chromatin* **10**, 6. doi:10.1186/s13072-017-0114-8

Kasper, D. M., Wang, G., Gardner, K. E., Johnstone, T. G. and Reinke, V. (2014). The C. elegans SNAPc component SNPC-4 coats piRNA domains and is globally required for piRNA abundance. *Dev. Cell* **31**, 145-158. doi:10.1016/j.devcel.2014.09.015

Langmead, B., Trapnell, C., Pop, M. and Salzberg, S. L. (2009). Ultrafast and memory-efficient alignment of short DNA sequences to the human genome. *Genome Biol.* **10**, R25. doi:10.1186/gb-2009-10-3-r25

Lee, H. C., Gu, W., Shirayama, M., Youngman, E., Conte, D., Jr. and Mello, C. C. (2012). C. elegans piRNAs mediate the genome-wide surveillance of germline transcripts. *Cell* **150**, 78-87. doi:10.1016/j.cell.2012.06.016

Makeyeva, Y. V., Shirayama, M. and Mello, C. C. (2021). Cues from mRNA splicing prevent default Argonaute silencing in C. elegans. *Dev. Cell* **56**, 2636-2648.e4. doi:10.1016/j.devcel.2021.08.022

Maniar, J. M. and Fire, A. Z. (2011). EGO-1, a C. elegans RdRP, modulates gene expression via production of mRNA-templated short antisense RNAs. *Curr. Biol.* **21**, 449-459. doi:10.1016/j.cub.2011.02.019

Marnik, E. A. and Updike, D. L. (2019). Membraneless organelles: P granules in Caenorhabditis elegans. *Traffic* **20**, 373-379. doi:10.1111/tra.12644

Montgomery, B. E., Vijayasarathy, T., Marks, T. N., Cialek, C. A., Reed, K. J. and Montgomery, T. A. (2021). Dual roles for piRNAs in promoting and preventing gene silencing in C. elegans. *Cell Rep.* **37**, 110101. doi:10.1016/j.celrep.2021.110101

Newman, M. A., Ji, F., Fischer, S. E. J., Anselmo, A., Sadreyev, R. I. and Ruvkun, G. (2018). The surveillance of pre-mRNA splicing is an early step in C. elegans RNAi of endogenous genes. *Genes Dev.* **32**, 670-681. doi:10.1101/gad.311514.118

Ni, J. Z., Chen, E. and Gu, S. G. (2014). Complex coding of endogenous siRNA, transcriptional silencing and H3K9 methylation on native targets of germline nuclear RNAi in C. elegans. *BMC Genomics* **15**, 1157. doi:10.1186/1471-2164-15-1157

Ni, J. Z., Kalinava, N., Chen, E., Huang, A., Trinh, T. and Gu, S. G. (2016). A transgenerational role of the germline nuclear RNAi pathway in repressing heat stress-induced transcriptional activation in C. elegans. *Epigenetics Chromatin* **9**, 3. doi:10.1186/s13072-016-0052-x

Ni, J. Z., Kalinava, N., Mendoza, S. G. and Gu, S. G. (2018). The spatial and temporal dynamics of nuclear RNAi-targeted retrotransposon transcripts in Caenorhabditis elegans. *Development* **145**, dev167346. doi:10.1242/dev.167346

Paix, A., Folkmann, A., Rasoloson, D. and Seydoux, G. (2015). High efficiency, homology-directed genome editing in caenorhabditis elegans using CRISPR-Cas9 ribonucleoprotein complexes. *Genetics* **201**, 47-54. doi:10.1534/genetics.115.179382

Phillips, C. M., Brown, K. C., Montgomery, B. E., Ruvkun, G. and Montgomery, T. A. (2015). piRNAs and piRNA-dependent siRNAs protect conserved and essential C. elegans genes from misrouting into the RNAi pathway. *Dev. Cell* **34**, 457-465. doi:10.1016/j.devcel.2015.07.009

Piatek, M. J. and Werner, A. (2014). Endogenous siRNAs: regulators of internal affairs. *Biochem. Soc. Trans.* **42**, 1174-1179. doi:10.1042/BST20140068

Pisacane, P. and Halic, M. (2017). Tailing and degradation of Argonaute-bound small RNAs protect the genome from uncontrolled RNAi. *Nat. Commun.* **8**, 15332. doi:10.1038/ncomms15332

Priyadarshini, M., Ni, J. Z., Vargas-Velazquez, A. M., Gu, S. G. and Frokjaer-Jensen, C. (2022). Reprogramming the piRNA pathway for multiplexed and transgenerational gene silencing in C. elegans. *Nat. Methods* **19**, 187-194. doi:10.1038/s41592-021-01369-z

Reed, K. J., Svendsen, J. M., Brown, K. C., Montgomery, B. E., Marks, T. N., Vijayasarathy, T., Parker, D. M., Nishimura, E. O., Updike, D. L. and Montgomery, T. A. (2020). Widespread roles for piRNAs and WAGO-class siRNAs in shaping the germline transcriptome of Caenorhabditis elegans. *Nucleic Acids Res.* **48**, 1811-1827. doi:10.1093/nar/gkz1178

Serizay, J., Dong, Y., Jänes, J., Chesney, M., Cerrato, C. and Ahringer, J. (2020). Distinctive regulatory architectures of germline-active and somatic genes in C. elegans. *Genome Res.* **30**, 1752-1765. doi:10.1101/gr.265934.120

Seth, M., Shirayama, M., Gu, W., Ishidate, T., Conte, D., Jr. and Mello, C. C. (2013). The C. elegans CSR-1 argonaute pathway counteracts epigenetic silencing to promote germline gene expression. *Dev. Cell* **27**, 656-663. doi:10.1016/j.devcel.2013.11.014

Seth, M., Shirayama, M., Tang, W., Shen, E.-Z., Tu, S., Lee, H.-C., Weng, Z. and Mello, C. C. (2018). The coding regions of germline mRNAs confer sensitivity to argonaute regulation in C. elegans. *Cell Rep.* **22**, 2254-2264. doi:10.1016/j.celrep.2018.02.009

Seydoux, G. (2018). The P granules of C. elegans: a genetic model for the study of RNA-protein condensates. *J. Mol. Biol.* **430**, 4702-4710. doi:10.1016/j.jmb.2018.08.007

Shen, E. Z., Chen, H., Ozturk, A. R., Tu, S., Shirayama, M., Tang, W., Ding, Y. H., Dai, S. Y., Weng, Z. and Mello, C. C. (2018). Identification of piRNA binding sites reveals the argonaute regulatory landscape of the C. elegans germline. *Cell* **172**, 937-951.e18. doi:10.1016/j.cell.2018.02.002

Sheu-Gruttadauria, J., Pawlica, P., Klum, S. M., Wang, S., Yario, T. A., Schirle Oakdale, N. T., Steitz, J. A. and MacRae, I. J. (2019). Structural basis for target-directed MicroRNA degradation. *Mol. Cell* **75**, 1243-1255.e7. doi:10.1016/j.molcel.2019.06.019

Shirayama, M., Seth, M., Lee, H. C., Gu, W., Ishidate, T., Conte, D., Jr. and Mello, C. C. (2012). piRNAs initiate an epigenetic memory of nonself RNA in the C. elegans germline. *Cell* **150**, 65-77. doi:10.1016/j.cell.2012.06.015

Shukla, A., Yan, J., Pagano, D. J., Dodson, A. E., Fei, Y., Gorham, J., Seidman, J. G., Wickens, M. and Kennedy, S. (2020). poly(UG)-tailed RNAs in genome protection and epigenetic inheritance. *Nature* **582**, 283-288. doi:10.1038/s41586-020-2323-8

Strome, S. and Wood, W. B. (1982). Immunofluorescence visualization of germ-line-specific cytoplasmic granules in embryos, larvae, and adults of Caenorhabditis elegans. *Proc. Natl. Acad. Sci. USA* **79**, 1558-1562. doi:10.1073/pnas.79.5.1558

van Wolfswinkel, J. C., Claycomb, J. M., Batista, P. J., Mello, C. C., Berezikov, E. and Ketting, R. F. (2009). CDE-1 affects chromosome segregation through uridylation of CSR-1-bound siRNAs. *Cell* **139**, 135-148. doi:10.1016/j.cell.2009.09.012

Vastenhouw, N. L., Brunschwig, K., Okihara, K. L., Müller, F., Tijsterman, M. and Plasterk, R. H. (2006). Gene expression: long-term gene silencing by RNAi. *Nature* **442**, 882. doi:10.1038/442882a

Wahba, L., Hansen, L. and Fire, A. Z. (2021). An essential role for the piRNA pathway in regulating the ribosomal RNA pool in C. elegans. *Dev. Cell* **56**, 2295-2312.e6. doi:10.1016/j.devcel.2021.07.014

Wang, Y., Weng, C., Chen, X., Zhou, X., Huang, X., Yan, Y. and Zhu, C. (2020). CDE-1 suppresses the production of risiRNA by coupling polyuridylation and degradation of rRNA. *BMC Biol.* **18**, 115. doi:10.1186/s12915-020-00850-z

Weick, E.-M., Sarkies, P., Silva, N., Chen, R. A., Moss, S. M., Cording, A. C., Ahringer, J., Martinez-Perez, E. and Miska, E. A. (2014). PRDE-1 is a nuclear factor essential for the biogenesis of Ruby motif-dependent piRNAs in C. elegans. *Genes Dev.* **28**, 783-796. doi:10.1101/gad.238105.114

Yang, A., Shao, T.-J., Bofill-De Ros, X., Lian, C., Villanueva, P., Dai, L. and Gu, S. (2020). AGO-bound mature miRNAs are oligouridylated by TUTs and subsequently degraded by DIS3L2. *Nat. Commun.* **11**, 2765. doi:10.1038/s41467-020-16533-w

Zhang, L., Ward, J. D., Cheng, Z. and Dernburg, A. F. (2015). The auxin-inducible degradation (AID) system enables versatile conditional protein depletion in C. elegans. *Development* **142**, 4374-4384. doi:10.1242/dev.129635

Zhou, X., Feng, X., Mao, H., Li, M., Xu, F., Hu, K. and Guang, S. (2017). RdRP-synthesized antisense ribosomal siRNAs silence pre-rRNA via the nuclear RNAi pathway. *Nat. Struct. Mol. Biol.* **24**, 258-269. doi:10.1038/nsmb.3376

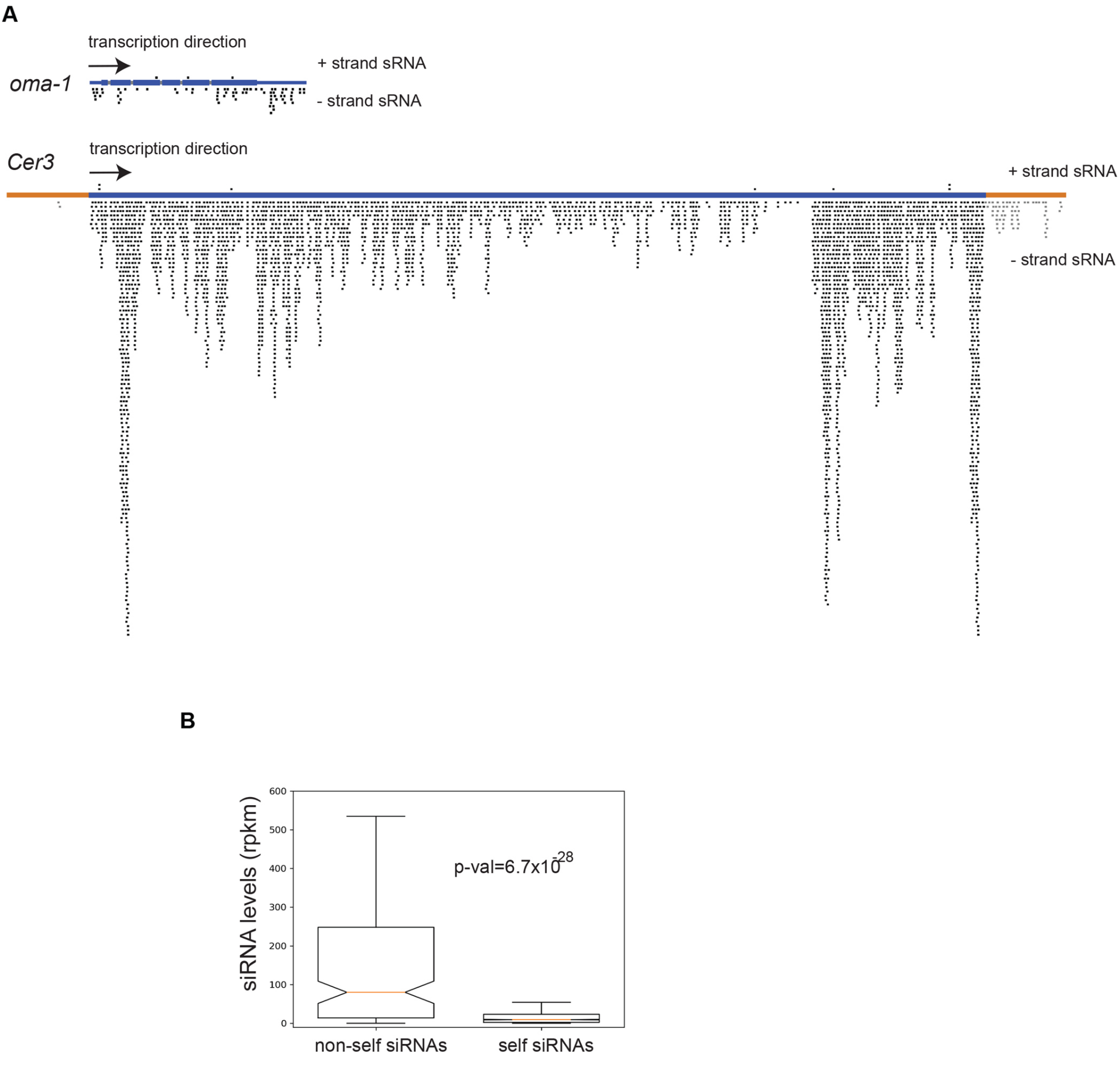

Fig. S1. Differential expression of self and non-self siRNAs. (**A**) siRNA track plots for *oma-1* and the LTR retrotransposon *Cer3* in WT adult animals from the same sequencing run. Each sequenced small RNA read is indicated as a black block above (sense sRNA) or under (antisense sRNA) the gene track. (**B**) Box plot of average siRNA levels of native germline nuclear RNAi targets (non-self siRNAs) and germline genes (self siRNAs) in WT animals. The native germline nuclear RNAi target genes were obtained from (Ni, Chen et al. 2014). The germline genes are the oogenic genes identified in (Ortiz, Noble et al. 2014).

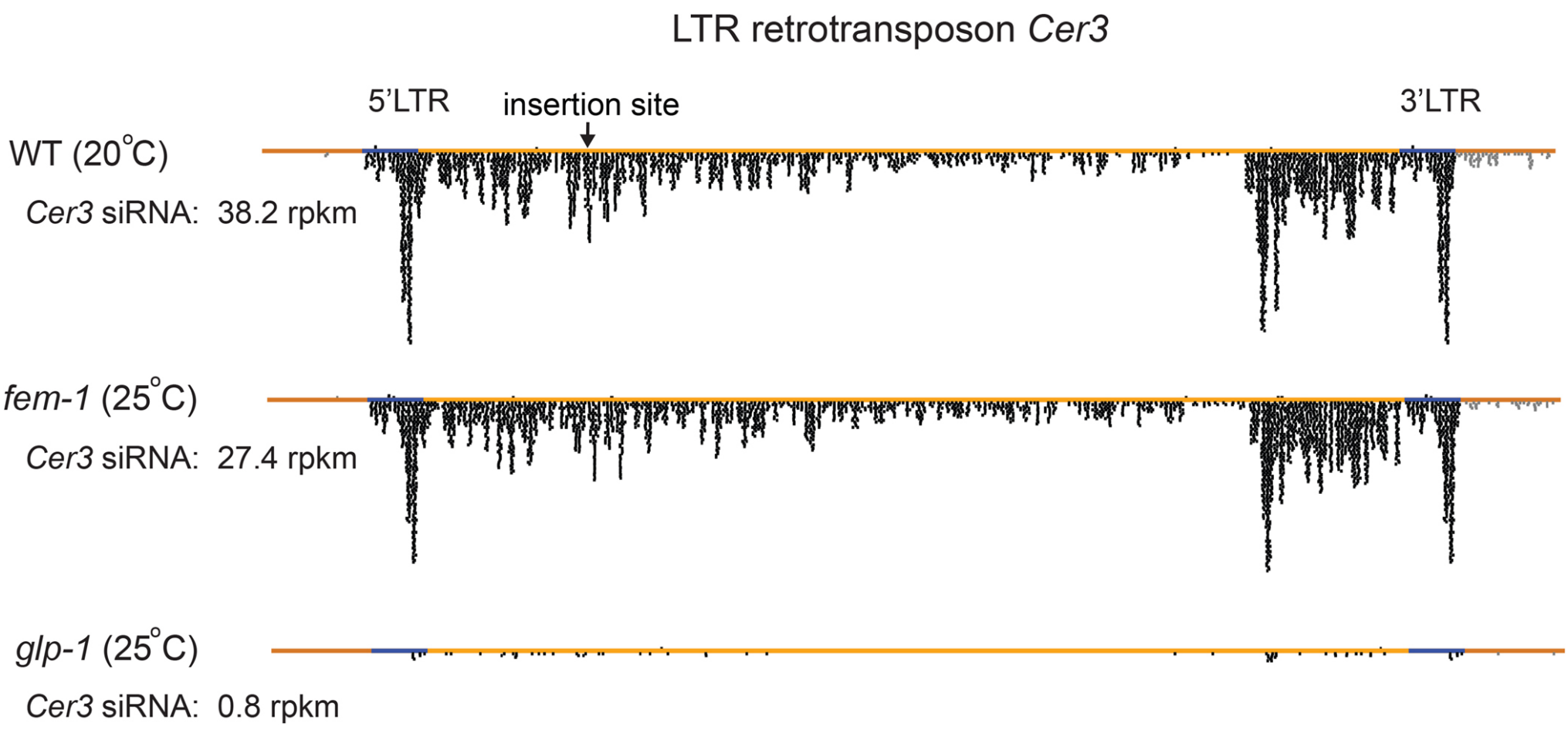

Fig. S2. Germline-enriched expression of *Cer3* siRNAs. *Cer3* siRNA track plots for adult WT (20°C), *fem-1*(*hc17*) (25° C, producing functional female germline, but lack of embryo in the uterus due to spermatogenesis defect) (Nelson, Lew et al. 1978), and *glp-1*(*e2141)* (25°C, germline depleted) (Kodoyianni, Maine et al. 1992) animals. As a quality control for the sRNA-seq, 30%, 12.7%, and 37% of sequenced small RNAs were mapped to microRNAs for WT, *fem-1*, and *glp-1*, respectively. The rpkm values of *Cer3* siRNAs are indicated in the figure. The insertion site in *Cer3* used in this study to express ectopic siRNAs is indicated.

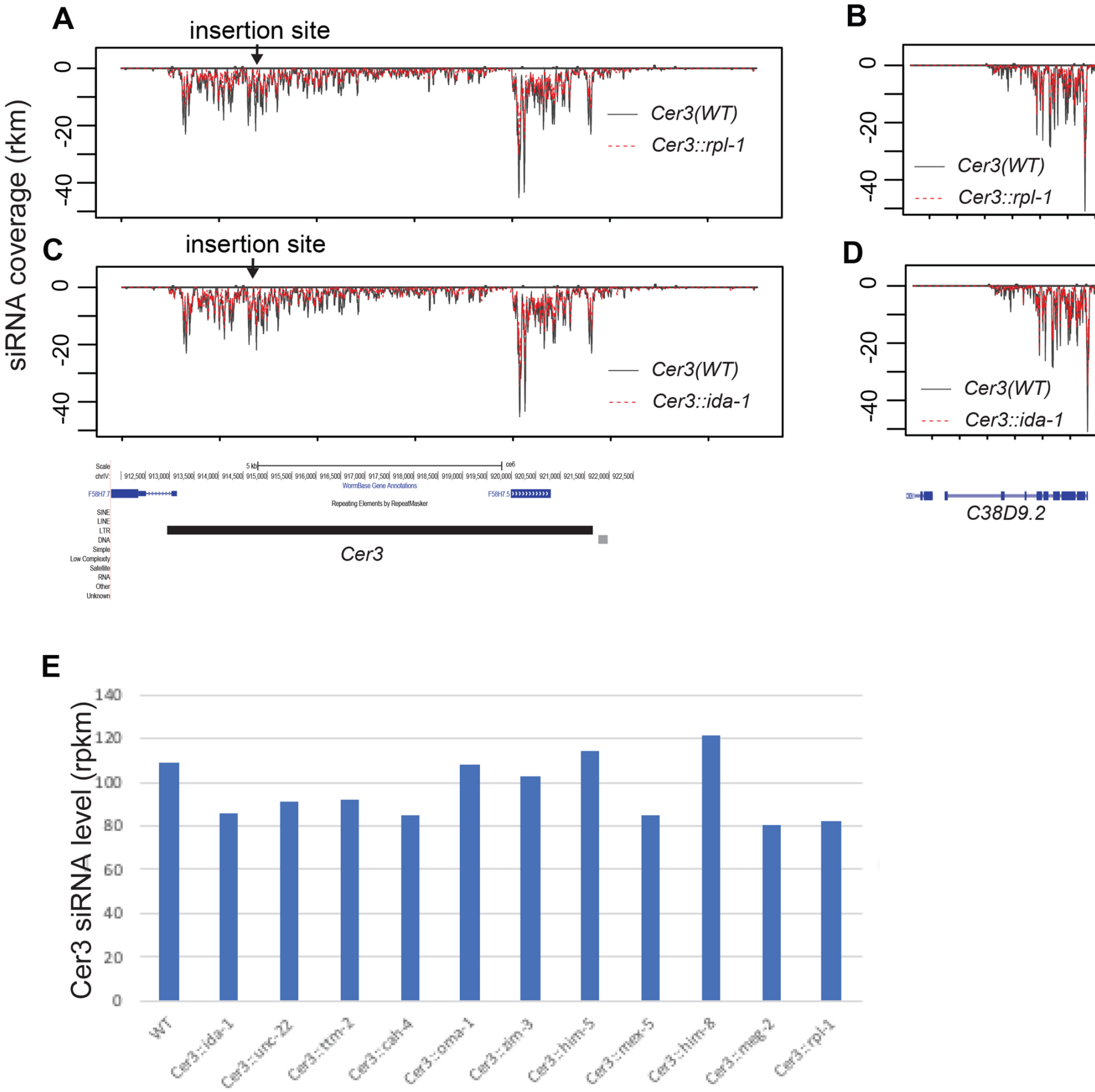

Fig. S3. *Cer3* siRNA expression is not affected by insertions. siRNA coverage plots at *Cer3* (**A** and **C**) and *c38d9.2* (**B** and **D**) are shown for strains carrying WT *Cer3*, *Cer3::rpl-1*, and *Cer3::ida-1* as indicated. Sense and antisense siRNA coverages are separately plotted as positive and negative values. siRNAs derived from the insertion were excluded from this analysis. The WT animals had slightly higher siRNA expressions than the two *Cer3* mutants for *Cer3* and other native nuclear RNAi targets, such as *c38d9.2* (**B** and **D**). This is likely due to a slight age difference between the samples (data not shown). (**E**) Bar graph showing Cer3 siRNA levels (rpkm) for WT and various *Cer3::insertion* mutant stains.

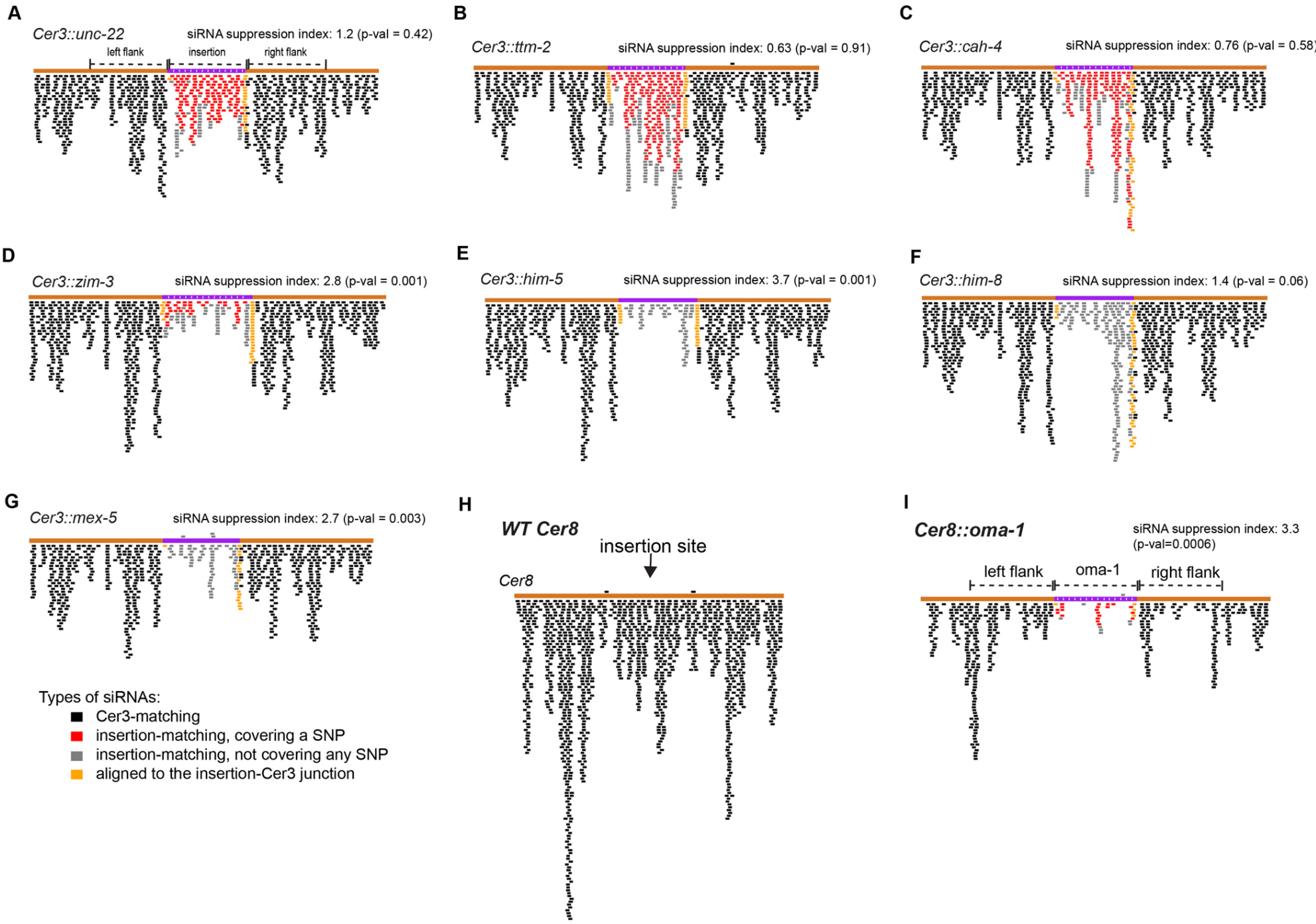

Fig. S4. siRNA track plots of additional *Cer3*::insertions (**A**-**G**), WT LTR retrotransposon *Cer8* (**H**), and *Cer8::oma-1* (**I**). Only the 700 nt *Cer8* sequence that flank each side of the insertion site is used for the plots. For *Cer3::him-5* (E), *Cer3::him-8* (F), and *Cer3::mex-5* (G), no SNPs were included in the insertion and therefore the insertion-matching siRNA reads were all colored in gray.

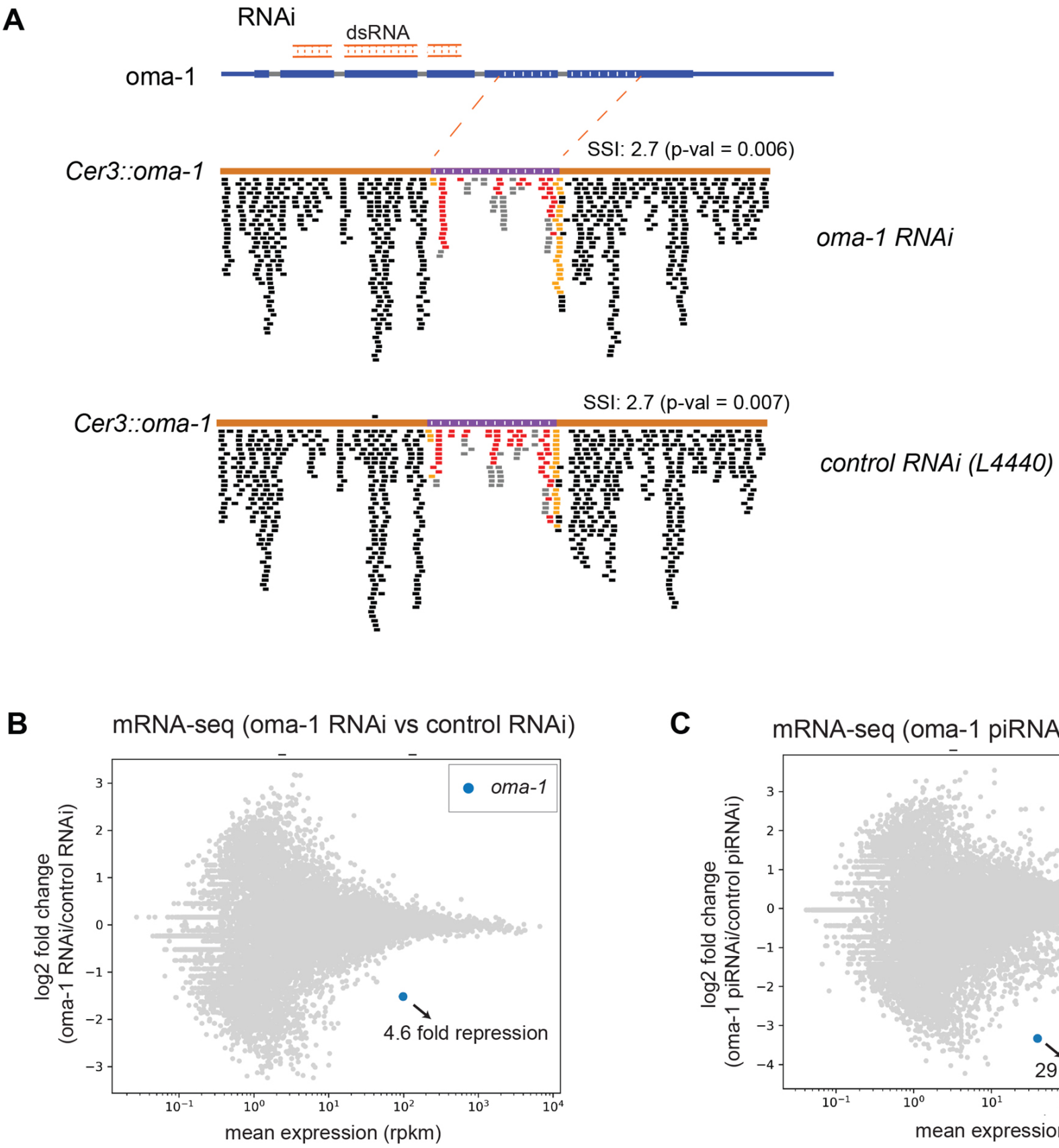

Fig. S5. *oma-1* RNAi did not affect siRNA suppression of *Cer3:oma-1*. (**A**): *Cer3::oma-1* siRNA track plot for *oma-1* RNAi or control RNAi (L4440 empty vector) animals. dsRNA targeted region in *oma-1* is indicated. (**B-C**): RNA-seq MA-plots of *oma-1* RNAi vs control (L4440) RNAi and *oma-1* piRNAi vs control (*unc-119*) piRNAi, showing that both *oma-1* dsRNA and piRNA led to *oma-1* mRNA repression, but the dsRNA-triggered repression was weaker than the piRNA-triggered repression.

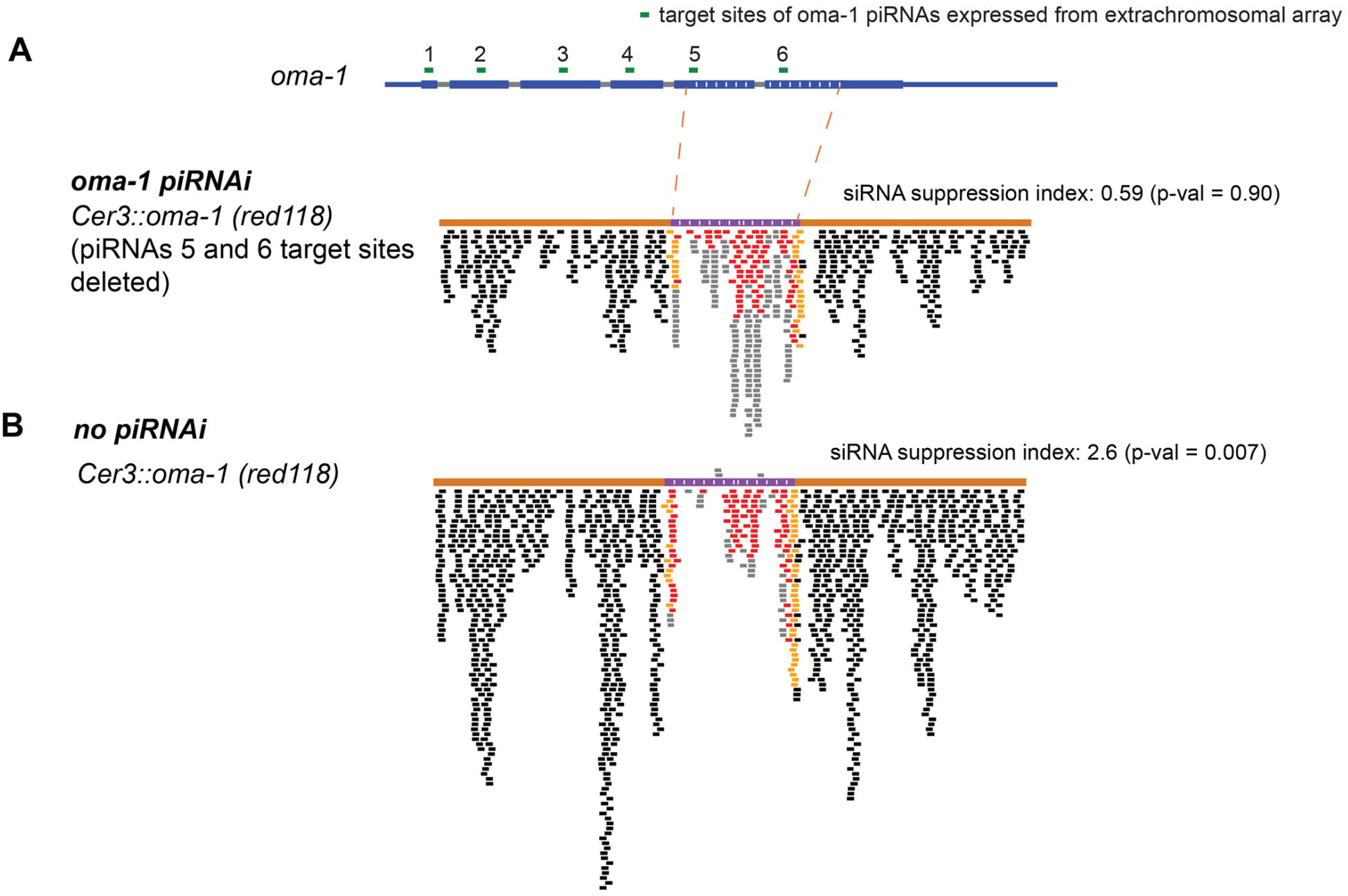

Fig. S6. Additional *oma-1* piRNAi experiments. The *oma-1* piRNAi transgene encodes six piRNAs. Their target sites in *oma-1* are indicated in (**A**). Two of the six piRNAs also target the *oma-1* fragment in *Cer3::oma-1* used in this study. To determine whether the effect of *oma-1* piRNAi on siRNA suppression was mediated by the piRNA target sites in the *Cer3::oma-1*, we generated a *Cer3::oma-1* allele (red118) that lacks these two target sites. The siRNA track plots with and without *oma-1* piRNAi are shown in **A** and **B**.

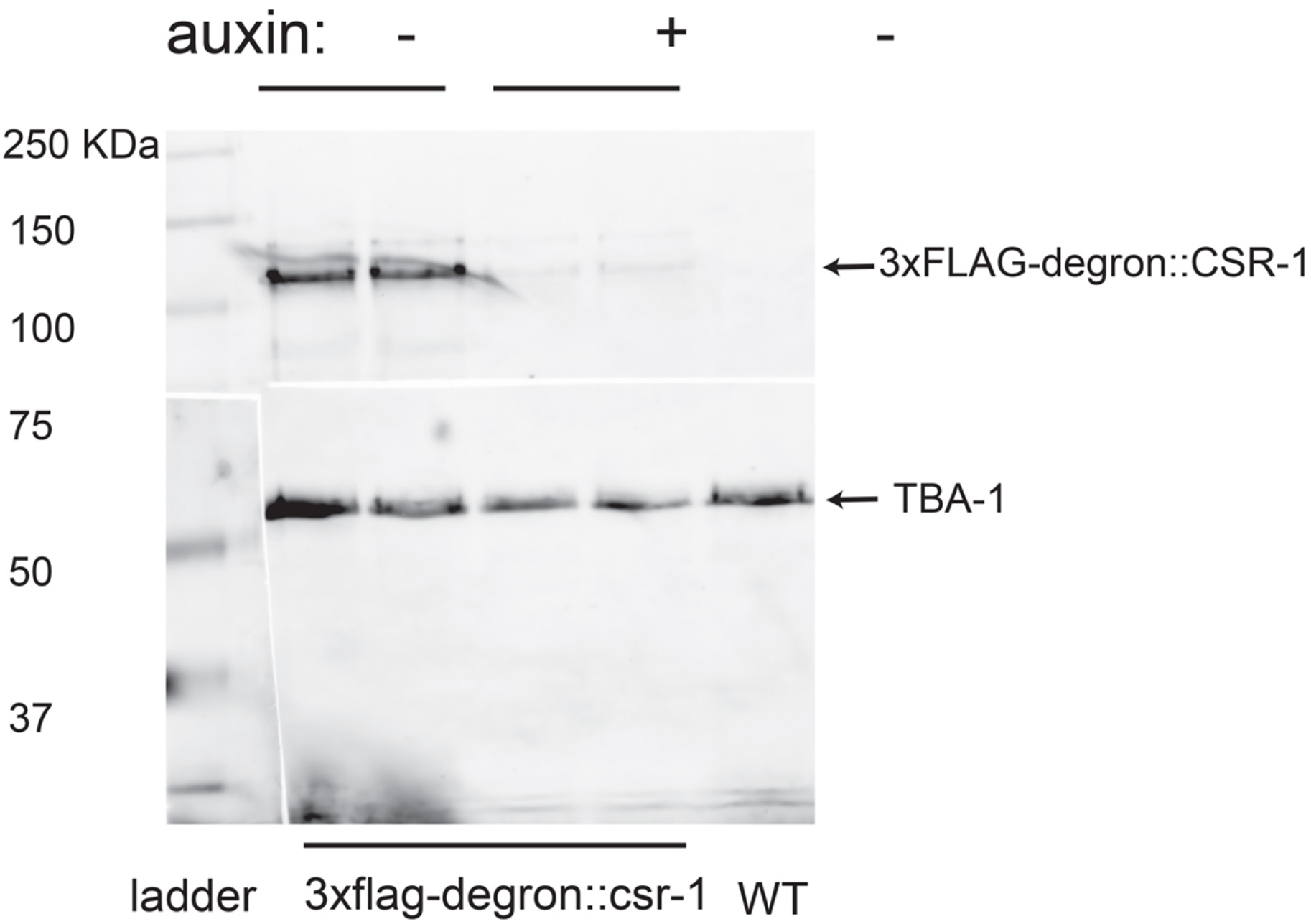

Fig. S7. Anti-FLAG western blot of 3xFLAG::degron::CSR-1 confirming auxin-induced degradation (AID) of CSR-1 (87% reduction). We note that, although the CSR-1 depletion was not complete, the animals exhibited a fully penetrant embryonic lethality, a phenotype expected for the loss-of-function *csr-1* mutation (data not shown).

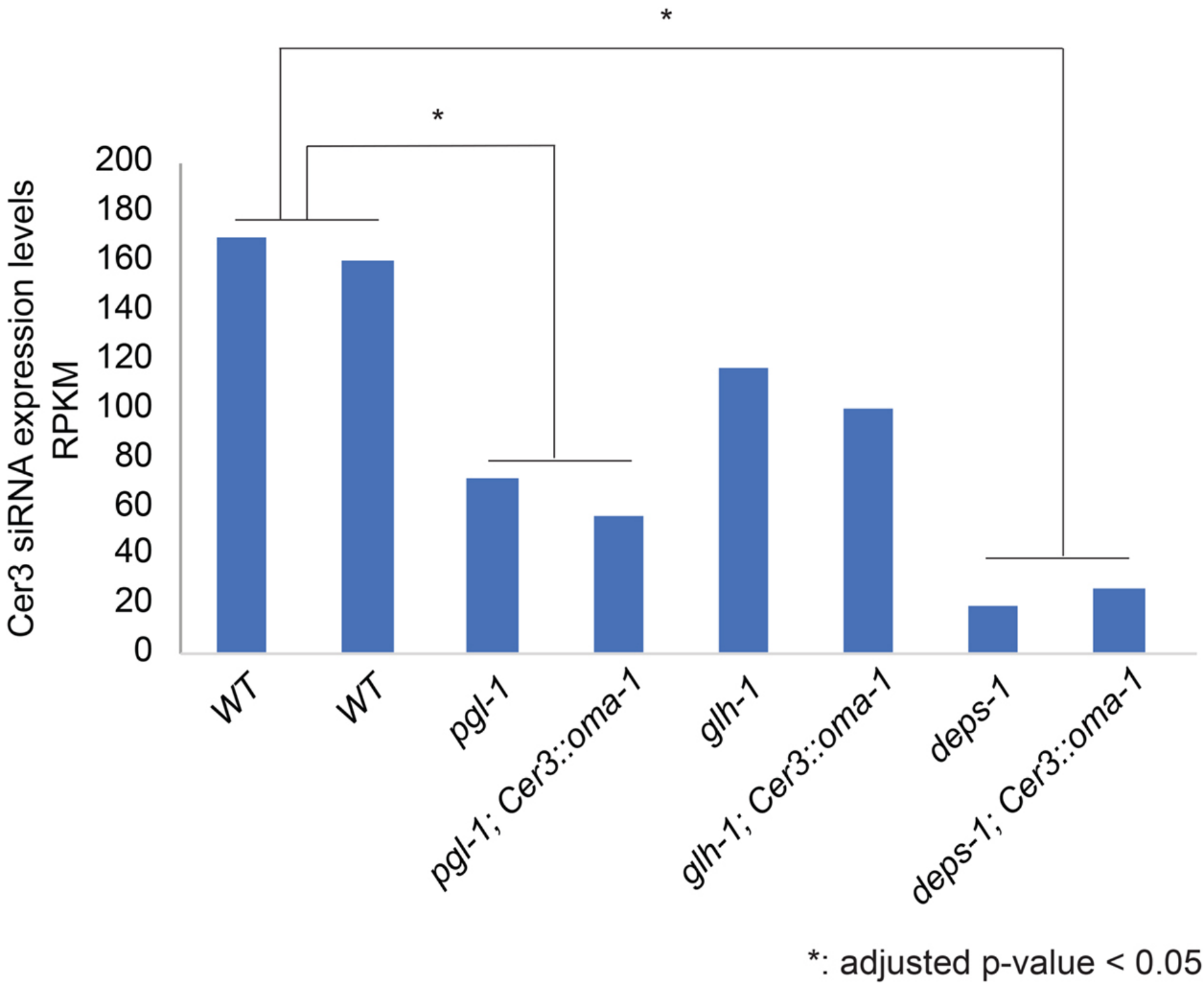

Fig. S8. *Cer3* siRNA expression levels in WT and P-granule mutant strains that carry either WT *Cer3* or *Cer3::oma-1*. The full-length WT *Cer3* sequence was used for the alignment to calculate the *Cer3* siRNA levels. DEseq2 (Love, Huber et al. 2014) was used to calculate the adjusted p-values for the comparison between WT and a mutant background. Both *pgl-1* and *deps-1* mutations were associated with significant reductions in *Cer3* siRNA production (3.7 and 9.2-fold reductions, respectively, adjusted p-values < 1.0×10^{-18}). A modest *Cer3* siRNA reduction was observed in the *glh-1* mutant animals (1.7-fold, adjusted p-values = 0.2).

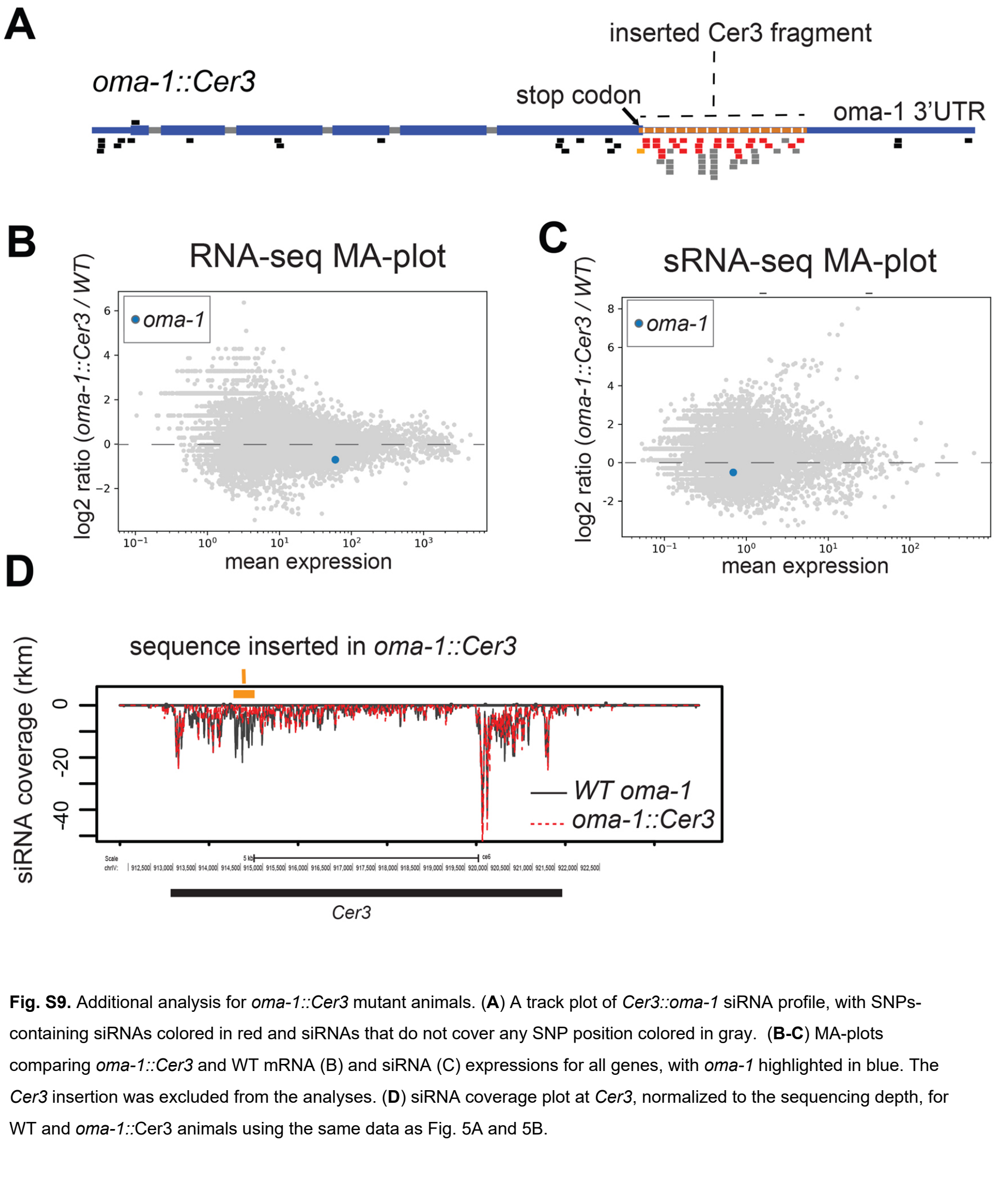

Fig. S9. Additional analysis for *oma-1::Cer3* mutant animals. (**A**) A track plot of *Cer3::oma-1* siRNA profile, with SNPs-containing siRNAs colored in red and siRNAs that do not cover any SNP position colored in gray. (**B-C**) MA-plots comparing *oma-1::Cer3* and WT mRNA (B) and siRNA (C) expressions for all genes, with *oma-1* highlighted in blue. The *Cer3* insertion was excluded from the analyses. (**D**) siRNA coverage plot at *Cer3*, normalized to the sequencing depth, for WT and *oma-1::*Cer3 animals using the same data as Fig. 5A and 5B.

Table S1. NGS libraries used in this study. All Fastq files have been deposited in NCBI with the GEO accession number GSE196847.

Click here to download Table S1

Supplementary Materials and Methods

DNA sequence of mutations created in this study:

1. Insertion site in Cer3 used in this study:

TCGGTTTCAAGACAGCCGCC[insertion]ACTTTGCCTCCGTTCAATGG

2. red20 (Cer3::oma-1), upper case: SNPs:

catgactaaCggtcgcattgcagctcccccgctttctgcGattcagcatcctttagaaatgtttgccagA
ccatcaactccagatgagccagcggctaaGttgccactaggaccaactcctgttagtacCcgtggtccaa
gatatgagctaccaacgaaAgaattgcatgacgcggaaggtgcgatgacTtatccaccgtctcgctggcc
attggatccGtcgatgtttgctctagacgcttggaatatggcCcatcggccagctagtccactcgattcA
atggttttgggttccgctccaaatgctggTtcgttcggaatgctcggaaagcaaaatacCcctggaggag
tttctggatattcatctgcCggatccacgccttctcaggatctcagttcCtcgtcactcaatgcagcat

3. red52 (Cer3::gfp), upper case: SNPs:

tccaatgcttctcccgtAacccagaccacatgaagcgtcacgacttcAtcaagtccgccatgccagaggg
atacgtcGaagagcgtaccatcttcttcaaggacgacCgaaactacaagacccgtgccgaggtcaagAtc
gagggagacaccctcgtcaaccgtatcCagctcaagggaatcgacttcaaggaggacCgtaacatcctgg
gacacaagctggagtacTactacaactcccacaacgtctacatcatgCccgacaagcaaaagaacggaat
caaggtcTacttcaagatccgtcacaacatcgaggacCgatcggtccaactcgccgaccactaccaaGaa
aacaccccaatcggtgacggaccagtcGtcctcccagacaaccactacctctccaccGaatccgccctct
ccaaggacccaaacgagTagcgtgaccacatggtcctcctcgagttcCt

4. red123(Cer3::rpl-1), upper case: SNPs:

agcaccatcttgacgaggctgccgccggaCacattccatcgatgagcgccgatgacttgTagaagcttaa
caagcagaagaagctcatcTagaagctcgccaagagctacgatgctttcTtcgcttccgaatccttgatc
aagcagatcGcacgtatcctcggtccaggactcaacaagCccggaaaattcccttccgtcgttacccacC
gagaatctctccaaagcaagagtgacgagTtccgcgccaccgtcaagttccagatgaagTaggttctctg
cctctccgtcgccgtcggtGacgttggactcacccaggaggagcttgtcAccaacatctccctctccatc
aacttcctcCtctcgctcttgaagaagaactggcagaacCtgagatcgtt

5. red124(Cer3::unc-22), upper case: SNPs:

gaggaagagcatgatgaatggttcagatgGaatcagaacccatctccaccaaataactaGaatgttccaa
atctcatcgacggaagaaaCtatagataccgagtatttgctgtcaatgaAgcaggactttccgatctagc
cgagcttgaAcaaactttgttccaagcatccggttctggTgaaggaccaaagattgtcagtccattgagG
gatttgaacgaagaagttggaagatgtgtGacatttgagtgtgaaatcagtggatctccTagacctgaat
acagatggttcaagggatgGaaggaacttgttgacaccagcaagtacacActtattaataagggagacaa
gcaagtcctAattatcaatgacttaacgtctgatgatgcAgatgaataca

6. red126(Cer3::ttm-2), upper case: SNPs:

tggaagtatcaaacagttagcgaaatgctAggattggatgtattctatgatgaaaatcaTaatcggcatt
tttcaagcgaatctgcatcAgcatcatcttcctctttattcacaacagcAgcaacatttcctattcaaat
tgaactaccAcattttgcacctccgagtttttattgcccTggatctccggtatccataaggttcacgttC
gaaatccaactttacaaccaaggatttaaTattgcatctcacgaagaaaatctcgtcgtTctaaattatg
aatctatcaaacggcaggtGactccgaagccggtcaattttcagaaaacAtttaactttccaaaggagcg
atcaatttcAttggaaatgctcctacctacagatgttttGacaactact

7. red127(Cer3::cah-4), upper case: SNPs:

ctggaacaccagctatgagtcgtttaatgAggcactcagcaagcccgatggattggcggAtgttggagtc
ttcttgaaggaaggaaaatTcaatgacaattaccatggcctgatcgacaGagtgcgcaaagccaccggaa
atgccacacGaattgccatgccaaaagacttccacattgTgcatcttctcccatccccggacaagagagT
attcgttacatacctcggatcccttaccaGcccaccatacaacgagtgtgttatctggaGcttgttcaca
gagcctgtggaggtctcctAcggacagctcaacgtgctccgtaatatcaAccccgccaatcatcgcgcct
gccaagacaCatgcgaccgtgaaatccgatcttccttcaTcttttaaatt

8. red47(Cer3::zim-3) , upper case: SNPs:

cttaacaagcgaaacgagcaaatgaataaGaatcatattattaaatgtaatttcgaaggCtgtaagcaaa
ttctctcgtggaaacttcgCtacggcaaacaacgacttctggatcatgcGatgactcatgaaaatgaaaa
gtgtctcgtCtgtcgcacatgtgaatactcttgcagtacGcatccccaaatgaagtatcactatcaaaaG
atgcatccagaagtgaggtgtgatgggttCaatattcagaaagtgttcaatatcgaattCgatgaagtgg
cgattttcgatcttttccaGaagtgcttcggagcacattcttccatcatAggaaatattgggaaaccgcg
gagatataaGaaatgtaaaaactcgctgaaaaatactccGgaagtcgacaatgagaatgtagataaagaT
tctccaggaccatcacacgatcttttctaCtttcgcagaattcgc

9. red145(Cer3::him-5):

cggtcgttcacagaacagaaatacatcgaaaaaaattgccgatggcccatatttttgccgagatacaga
attcgagacaatgcagagagatcagtaggtgcacgtttcaagagtcttccacaaaaagaacaagacgaag
tagtgaatgaagctttttcgaatcttcgagaatatttgaaaaagagggaacctttctatgcaaagctccg
gaaagctaactccaagtattcctcaaagcccaaagaaagagaaaaatctgtcgactccaatgacgaagct
gatagacgcaataagggaaataagaaaactcaaaaaaatgcgagtaagaactgccaaattgagaaatcgt
cgaataattctggaattctcaaaaaaagtggatcaggaatcagcgtggcttcta

10. red146(Cer3::him-8):

cggtgtagacaacgatggaaatattgatgattatgaagagtatcagtcattaccaccgaatgatgatgtt
attatgaatgaaacagaattgatggatgttgatcgaaccacagtgatgactccattacgaagtcctacat
ttttcgattatcacaacgaatccggtgatgaagatcagttgaatgagaatgaaatgaaatctccagacag
caaaaacgacgagattaataaagatgaaatccacaatattcaatgtcatttcccgaactgcaatcgagca
attgcgtggaagaggaaatatggaaaacttcgtcttatcgatcacgcattggtccattgcgataaaaact
ttctgaaatgcaaaaaatgcaagcacacttgtcatacaatccgtcaaatgcg

11. red147a(Cer3::mex-5):

caccttgacaatcacaacgatgacacgatgagcgctgaaaaggaaaatcatttccatgaacatcgtggc
gagaagttcggtcgtcgtggattcccaattccagaaactgacagtcaacaaccacccaactacaagactc
gtctttgcatgatgcacgcatctggaatcaaaccatgtgatatgggtgctcgatgcaagtttgctcatgg
gctcaaagagctcagagctactgatgctccggctcgctatccgaacaacaagtacaagacaaagctgtgc
aagaactttgcgcgtggaggaactggattctgcccgtatggacttcgttgcgagtttgttcatccaacgg
acaaggaattccagaatattcctccatatcagcgcatgtctc

12. red40 (Cer3::oma-1), upper case: SNPs:

atgctgcattgagtgacgaGgaactgagatcctgagaaggcgtggatccGgcagatgaatatccagaaac
tcctccaggGgtattttgctttccgagcattccgaacgaAccagcatttggagcggaacccaaaaccatT
gaatcgagtggactagctggccgatgGgccatattccaagcgtctagagcaaacatcgaCggatccaatg
gccagcgagacggtggataAgtcatcgcaccttccgcgtcatgcaattcTttcgttggtagctcatatct
tggaccacgGgtactaacaggagttggtcctagtggcaaCttagccgctggctcatctggagttgatggT
ctggcaaacatttctaaaggatgctgaatCgcagaaagcgggggagctgcaatgcgaccGttagtcatg

13. prg-1(red115), upper case: WT sequence, lower case: mutation :
TTATTCTATCAGCCCGCTCAgctagctGTGAATTCGTGAAGGATGGG

14. prde-1(red139), upper case: WT sequence, lower case: mutation :
GCATCGATTCACCGATGAGGgctagcaACTTttCAGGTCTGAAGGAGCAAAAG

15. pgl-1(red116), upper case: WT sequence, lower case: mutation :
AAGTTGTGAACCATATCGCTtAAgCTagcTTTCGAGGAAGCGAGTAAAA

16. glh-1(red117), upper case: WT sequence, lower case: mutation :
TGAATGTCCGGAGCCACCCCGcTaGctGATGTTTCAATTGTGGCGAG

17. oma-1(red57), oma-1::Cer3 , upper case: oma-1 sequence with stop codon underlined, lower case: Cer3 insertion (with SNPs indicated in the upper case):
TGACCAAGCATCTCAATTGAaccccaagaAacgtgttgtctggaagcagtgcaggtagtGacgctactga
ctcttctggaagtggatccTcgatgccatcgagtctccagaatcgtgacAtcgtcgaagaacaatcggaa
gatcagcaaTtcaatagtggtgagcttgcgggagatcaaAatgatctagaagaagcaacaaattcaattT
gtggaatttcgccttcaattggagtgatcAgtttcaagacagccgccactttgcctccgCtcaatggaaa
cttgactgaagatttcacaGccttcgtgcgaaagttcaaggatcggctaAcagcgtctacagagatggac
aacgatcaaGagaggtctacattccttttatttttggacGatcgcgcgcggagtacggccgatggaataG
ttggagcacagcctgcgattacactcgagAatcttatcacaaagatgtcagcagtgttcAagaatgcTTG
TGGTGAACAACTTCTCT

18. Cer8(red35), Cer3::oma-1, upper case: Cer8 sequence, lower case: oma-1 insertion (with SNPs indicated in the upper case):

CCATTTGAAGAAATCCAAGTcatcatgactaaCggtcgcattgcagctcccccgctttctgcGattcagc
atcctttagaaatgtttgccagAccatcaactccagatgagccagcggctaaGttgccactaggaccaac
tcctgttagtacCcgtggtccaagatatgagctaccaacgaaAgaattgcatgacgcggaaggtgcgatg
acTtatccaccgtctcgctggccattggatccGtcgatgtttgctctagacgcttggaatatggcCcatc
ggccagctagtccactcgattcAatggttttgggttccgctccaaatgctggTtcgttcggaatgctcgg
aaagcaaaatacCcctggaggagtttctggatattcatctgcCggatccacgccttctcaggatctcagt
tcCtcgtcactcaatgcagcatCATCGCCTGAGTAGTGCAGC

19. red118 (Cer3::oma-1), upper case: SNPs:

attgcagctcccccgctttctgcGattcagcatcctttagaaatgtttgccagAccatcaactccagatg
agccagcggctaaGttgccactaggaccaactcctgttagtacCcgtggtccaagatatgagctaccaac
gaaAgaattgcatgacgcggaaggtgcgatgacTtatccaccgtctcgctggccattggatccGtcgatg
tttgccCcatcggccagctagtccactcgattcAatggttttgggttccgctccaaatgctggTtcgttc
ggaatgctcggaaagcaaaatacCcctggaggagtttctggatattcatctgcCggatccacgccttctc
aggatctcagttcCtcgtcactcaatgcagcat

Reference:

Kodoyianni, V., E. M. Maine and J. Kimble (1992). "Molecular basis of loss-of-function mutations in the glp-1 gene of Caenorhabditis elegans." *Mol Biol Cell* **3**(11): 1199-1213.
Love, M. I., W. Huber and S. Anders (2014). "Moderated estimation of fold change and dispersion for RNA-seq data with DESeq2." *Genome Biol* **15**(12): 550.
Nelson, G. A., K. K. Lew and S. Ward (1978). "Intersex, a temperature-sensitive mutant of the nematode Caenorhabditis elegans." *Dev Biol* **66**(2): 386-409.
Ni, J. Z., E. Chen and S. G. Gu (2014). "Complex coding of endogenous siRNA, transcriptional silencing and H3K9 methylation on native targets of germline nuclear RNAi in C. elegans." *BMC Genomics* **15**: 1157.
Ortiz, M. A., D. Noble, E. P. Sorokin and J. Kimble (2014). "A new dataset of spermatogenic vs. oogenic transcriptomes in the nematode Caenorhabditis elegans." *G3 (Bethesda)* **4**(9): 1765-1772.